Master's Thesis
석사 학위논문

Synthesis and Characterization of Polymers based on Benzimidazole Segments for Polymer Solar Cells

Hayoung Kim(김 하 영 金 荷 英)

Department of Energy Systems Engineering

에너지시스템공학 전공

DGIST

2013

Master's Thesis
석사 학위논문

Synthesis and Characterization of Polymers based on Benzimidazole Segments for Polymer Solar Cells

Hayoung Kim(김 하 영 金 荷 英)

Department of Energy Systems Engineering

에너지시스템공학 전공

DGIST

2013

Synthesis and Characterization of Polymers based on Benzimidazole Segments for Polymer solar Cells

Advisor : Professor Youngu Lee

Co-advisor : Doctor Dae-Hwan Kim

by

Hayoung Kim

Department of Energy Systems Engineering

DGIST

A thesis submitted to the faculty of DGIST in partial fulfillment of the requirements for the degree of Master of Science in the Department of Energy Systems Engineering. The study was conducted in accordance with Code of Research Ethics[1]

12. 05. 2012

Approved by

Professor Youngu Lee (Signature)
(Advisor)

Doctor Dae-Hwan Kim (Signature)
(Co-Advisor)

[1] Declaration of Ethical Conduct in Research: I, as a graduate student of DGIST, hereby declare that I have not committed any acts that may damage the credibility of my research. These include, but are not limited to: falsification, thesis written by someone else, distortion of research findings or plagiarism. I affirm that my thesis contains honest conclusions based on my own careful research under the guidance of my thesis advisor.

Synthesis and Characterization of Polymers based on Benzimidazole Segments for Polymer solar Cells

Hayoung Kim

Accepted in partial fulfillment of the requirements for the degree of Master of Science

12. 05. 2012

Head of Committee _____(인)
Prof. Youngu Lee

Committee Member_____(인)
Dr. Dae-Hwan Kim

Committee Member_____(인)
Prof. Seung-Tae Hong

MS/ES
201124004

김 하 영. Hayoung Kim. Synthesis and Characterization of Polymers based on Benzimidazole Segments for Polymer Solar Cells. Department of Energy Systems Engineering. 2012. 42p. Advisors Prof. Lee, Youngu. Co-Advisors Dr. Kim, Dae-Hwan.

ABSTRACT

To enhance performance of polymer solar cells, a series of polymers which were based on electron-deficient benzimidazole segments and electron-rich benzodithiophene segments for polymer solar cells were designed and synthesized by the Stille polycondensation. The synthesized polymers which had long alkyl side chain exhibited good solubility in organic solvents. The optical and electrochemical properties of polymers were measured by UV/Vis spectroscopy and cyclic voltammetry (CV). The resulting polymers exhibited low optical bandgaps and electrochemical bandgaps. Furthermore, HOMO and LUMO energy levels of -3.4 ~ 6.0 eV were suitable for photovoltaic applications. These HOMO and LUMO energy levels are appropriate for charge transport to achieve high performance of polymer solar cells. The optical and electrochemical properties were tuned by introducing different substituents and alkyl side chains on benzimidazole segments. The polymer solar cells with benzimidazole based polymer achieved power conversion efficiency close to 1% due to their enhanced light harvesting property and efficient interpenetrating network which were caused by a hydrogen atom on benzimidazole segment and a lack of long alkyl side chain. This work implies that the electron-deficient benzimidazole segments based polymers can achieve high PCE through structural modification of the polymer.

Keywords: polymer solar cells, benzimidazole, benzodithiophene, donor-acceptor structure, conjugated polymers

CONTENTS

LIST OF FIGURES

LIST OF TABLES

LIST OF SCHEMES

1. INTRODUCTION

Polymer solar cells (PSCs) have attracted a considerable attention because of their advantages of light weight, flexibility, and low costs of materials, easy fabrication process [1]. PSCs can be fabricated by solution technology such as printing, roll-to roll technologies which are simple and low cost production process. The bulk heterojunction structure for PSCs is composed of a phase-separated blend of electron-donor units such as p-type conjugated polymers and electron-acceptor units such as n-type fullerene derivatives. Generally, poly(3-hexylthiophene) (P3HT) has been used as an electron-donor material for PSCs because it can absorb sunlight in the range of visible wavelength. Fullerene derivatives such as [6,6]-phenyl-C61-butyric methyl ester ($PC_{61}BM$) or [6,6]-phenyl-C71-butyric methyl ester ($PC_{71}BM$) have been used as n-type materials due to their superior electron-accepting and electron-transporting properties. So far, the PSCs based on P3HT and $PC_{61}BM$ showed power conversion efficiency (PCE) up to 5% [2]. However, PSCs with P3HT and PCBM exhibited still lower efficiency than conventional silicon solar cells. Since the optical bandgap of P3HT is 1.85 eV, it absorbs only 45% of solar spectrum [3]. Therefore, it is necessary to develop new types of electron-donor polymers to achieve high PCEs. The electron-donor polymers need to possess several characteristics such as harvesting photons in a wide range of spectrum, efficient exciton dissociation, suitable HOMO and LUMO energy levels, and good miscibility with the electron-acceptor materials [4]. The electron-donor polymers should have air stability and high hole mobility for efficient charge transport in a solar cell [5]. Furthermore, the electron-donor polymers need to be highly soluble in common organic solvents for solution process such as spin coating, spray coating, screen printing, or ink-jet printing [6]. To obtain these characteristics for the electron-donor polymers, various donor-acceptor types of copolymers which contain donor and acceptor segments alternatively in polymer backbone have been designed and synthesized [4]. Generally, the donor-acceptor polymers exhibit low optical bandgaps due to intramolecular charge transfer reaction between donor and acceptor segments. For example, electron-deficient benzothiadiazole has been used as an acceptor segment to

afford copolymers with various electron-rich segments [7]. One of drawbacks of benzothiadiazole is the synthetic difficulty in modifying chemical structures for tuning the optoelectronic properties of the polymers. Various benzimidazole derivatives have been used as electron injecting and transporting materials in organic light-emitting diodes (OLEDs) because of their high electron accepting and transporting properties. In addition, the optoelectronic properties of the benzimidazole segments can be easily tuned by introducing various functional groups [8, 9].

In this paper, a series of copolymers with benzodithiophene segments as donor units and benzimidazole segments as acceptor units was synthesized and characterized for development of efficient PSCs. The physical properties of the polymers were tuned by the structural variation of the polymer with different side alkyl chains and substituents. The optical and electrochemical properties of the polymers were characterized by UV/Vis spectroscopy and cyclic voltammetry. It was found that the polymers exhibit low bandgaps and suitable HOMO and LUMO energy levels for PSCs. The bulk heterojunction solar cell devices with the polymers showed power conversion efficiency (PCE) close to 1%. This study will provide more opportunities for development of new class of materials for polymer solar cells which can achieve high PCEs.

2. THEORETICAL BACKGROUND

2.1. Principle and Characters of Polymer Solar Cells

The operation process of converting sunlight into electric current in a polymer solar cell is composed of four processes [10, 11].

(ⅰ) Absorption of a photon and generation of the electron-hole pair which is called as exciton

(ⅱ) Diffusion of exciton

(ⅲ) Exciton dissociation by charge transfer

(ⅳ) Charge transport and collection to electrode

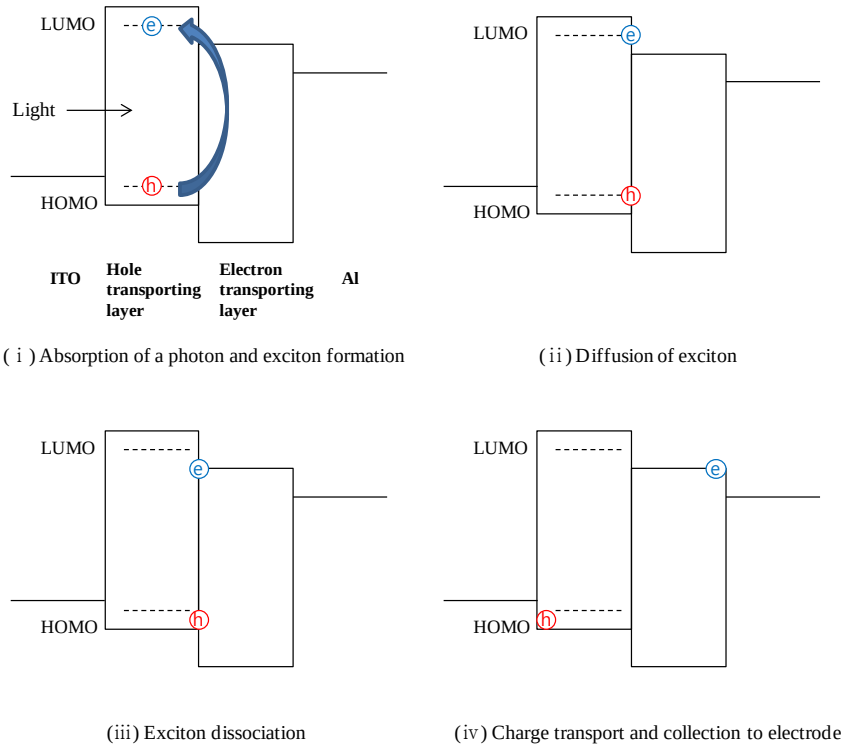

(ⅰ) Absorption of a photon and exciton formation

(ⅱ) Diffusion of exciton

(ⅲ) Exciton dissociation

(ⅳ) Charge transport and collection to electrode

Figure 2.1. The operation process of polymer solar cells.

As shown in Figure 2.1, sunlight is absorbed inside the solar cell device, and then electron in HOMO level is excited to LOMO level of donor material. The excited electron forms the exciton which is electron-hole pair. The exciton diffuses inside of the organic semiconductor. Typically, the exciton diffusion length is around 10 ~ 20 nm. The exciton dissociation takes place at the region between the donor and acceptor materials [12, 13]. To generate electric power, the exciton must be dissociated and collected at electrode. If exciton does not reach the interface between the donor and acceptor materials, electron and hole will be recombined and dissipated without generating photocurrent [11].

When the inorganic solar cells absorb photon, electron in the p-type semiconductor is excited to the valance band from conduction band. The excited electron generates the electron-hole pair at the p-type semiconductor. And then, the electron-hole pair moves to the n-type semiconductor by electric field that exists at p-n junction. The electric field performs as a role to separate electron-hole pair. Therefore, the electrons which exist in the n-type semiconductor move to the p-type semiconductor at the p-n junction. The holes which are in the p-type semiconductor diffuse to the n-type semiconductor. The empty places where electrons and holes are removed will have cations and anions. At this time, difference voltage is generated [14, 15].

Compared with inorganic semiconductor, organic semiconductors have higher absorption coefficient which affects to enhance light absorption in even 100nm thin film devices [10]. Another difference between the organic and inorganic semiconductors is dielectric constant. The electrostatic attractive force between the hole and the electron which is coulomb attraction is proportional to $1/\varepsilon$ (ε=3, dielectric constant). In the organic semiconductors, charge separation is more difficult because of their low dielectric constant. In the inorganic semiconductors, photon generates free electron and hole, whereas the exciton is formed in the organic semiconductor [16, 17]. For dissociation of exciton, strong electric fields are required. Under the electric fields, the exciton is dissociated into free charge carriers which are hole and electron. In the inorganic semiconductors, the coulomb attraction can be neglected due to the larger dielectric constant. However, the organic semiconductors need exceeding energy, which is higher than binding energy between electron and hole of 0.4 eV, to separate the

exciton. The organic semiconductors have higher extinction constant than that of the inorganic semiconductor. Therefore, the organic semiconductors can absorb enough light with about 300 nm film thick. Because hole mobility of organic semiconductor is low, polymer solar cell must have the optimized thickness of less than 100 nm [10, 13].

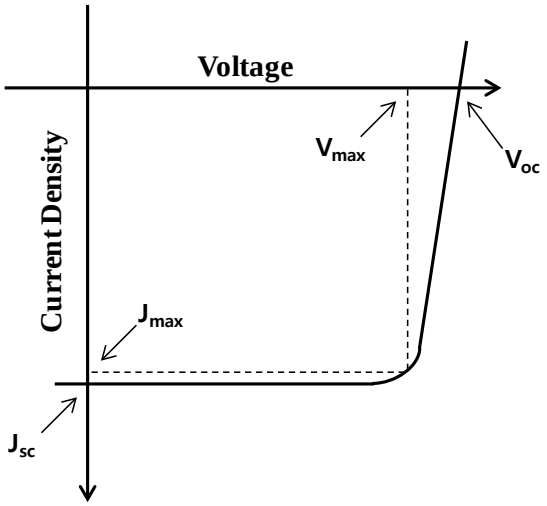

Figure 2.2. Typical current-voltage curve of polymer solar cells.

$$\eta_e = \frac{V_{oc} \times J_{sc} \times FF}{P_{in}} \qquad (1)$$

The photovoltaic power conversion efficiency (η_e) is defined by above equation (1). V_{oc} is the open circuit voltage, and J_{sc} is the short circuit current. FF means fill factor, and P_{in} indicates incident light power. P_{in} is standardized at 100 mW/cm^2 and under AM 1.5G condition. I_{max} and V_{max} are maximum power point of current and voltage in the fourth quadrant [19].

V_{oc} indicates applied voltage, and the maximum voltage difference attainable between the two electrodes. V_{oc} corresponds to the voltage when the current under illumination is zero. V_{oc} of organic semiconductor is typically 0.5 ~ 1.5 V that is higher value than V_{oc} of inorganic semiconductor [16]. The bandgap of active layer gives the thermodynamic limit that reduces V_{oc} [19]. At the organic solar cells, V_{oc} is limited by energy difference between HOMO of the donor and the LUMO of the acceptor

[20]. Also, V_{oc} is dependants on LUMO position of acceptor, such as fullerene derivative, and weakly dependant on the metal workfunction which is used as the negative electrode [21, 22].

When the voltage in the cell is zero, the maximum current is called J_{sc}. J_{sc} is determined by the amount of absorption light and the internal conversion efficiency. Therefore, the low bandgap donor polymer is necessary to enhance J_{sc} because the low bandgap polymer enhances light absorption. In AM 1.5G condition, the maximum irradiance energy is at ~500 nm and the maximum photon flux is at ~670 nm. Hence, the organic semiconductors have to absorb the photons at the maximum irradiation. Furthermore, it must have a broad absorption spectrum and high absorption coefficient to enhance J_{sc}. J_{sc} indicates the charge separation and transport efficiency in the solar cell [23].

$$FF = \frac{J_{max} \times V_{max}}{J_{sc} \times V_{oc}} \qquad (2)$$

FF is described by above equation (2). FF implies quality of the device, and it is around 0.4 ~ 0.6. FF influences shunt and series resistance. To get higher FF, the shunt resistance should be considerably large to prevent current leakage. In addition, series resistant should be low to get a sharp rise in the forward current [10].

2.2. Structures of Polymer Solar Cells

The first attempted structure of organic solar cell was single organic layers which are sandwiched between two metal electrodes that have difference work function [25]. In this structure, the photovoltaic properties of organic solar cells are dependent on the character of the electrodes. The characters of single layer device are caused by the asymmetry in the electron and hole injection into the molecular π and π^* orbital. The power conversion efficiency of single layer organic solar cell was reported as the poor efficiency of 0.7%.

In 1986, the bilayer structure was introduced to organic semiconductor. In the bilayer structure, two organic layers which have specific electron or hole transporting characters are sandwiched between a transparent conducting oxide (ITO) electrode for collecting of the positive charge and a semitransparent metal (Ag) electrode for collecting the negative charges [26]. Copper phthalocyanine was used as electron donor, and perylene tetracarboxylic derivatives were used as electron acceptor. The bilayer heterojunction structure achieved the power conversion efficiency of 1%. The exciton dissociation occurs at the interface between the electron donor and acceptor layer. The exciton diffusion length is 10 nm. Therefore, sunlight should be absorbed within a thin layer around interface. It means that the thickness of active layer limits efficiency of the bilayer structure.

Most organic solar cells have the active layer below 100 nm to absorb the most of sunlight despite short exciton diffusion length of 10 nm. The thicker active layer can absorb more light, but only a small amount of exciton will reach the interface and dissociate [16]. The bulk heterojunction structure, which is blended structure of donor and acceptor materials, can absorb more light, and help the dissociation of many excitons. The bulk heterojunction structure is similar with the bilayer structure. However, the donor and acceptor materials well dispersed throughout the bulk and lead to a three dimensional bulk heterojunction. Therefore, it develops the large interface area where exciton dissociates and charges can separate to electron and hole within lifetime of excitons. Furthermore, charge recombination is reduced and the current will follow the light intensity [26, 27]. In the case of

the bilayer structure, the donor and acceptor layers contact with the anode and cathode separately. On the other hand, the blend of donor and acceptor in the bulk heterojunction contact with electrode for pathway which transports hole and electron.

An important issue for blending of donor and acceptor materials is miscibility. Increasing the miscibility of the acceptor and donor can decrease the ratio of donor and acceptor, and enhance the optical density.

To achieve high performance of polymer solar cells, the blended donor and acceptor materials have to form a bicontinuous and interpenetrating network [10]. It means that the bulk heterojunction is more sensitive to nanoscale morphology in the blend [28]. The separating phase of component materials and the interfacial energy which makes high surface area are necessary for forming interpenetrating networks.

The bulk heterojunction was proposed in 1995 by Yu et al. The first bulk heterojunction device achieved power conversion efficiency of about 1% [29]. Although the bulk heterojunction device reported low efficiency, it achieved over 3% of efficiency by engineering and improvement of device [30, 31].

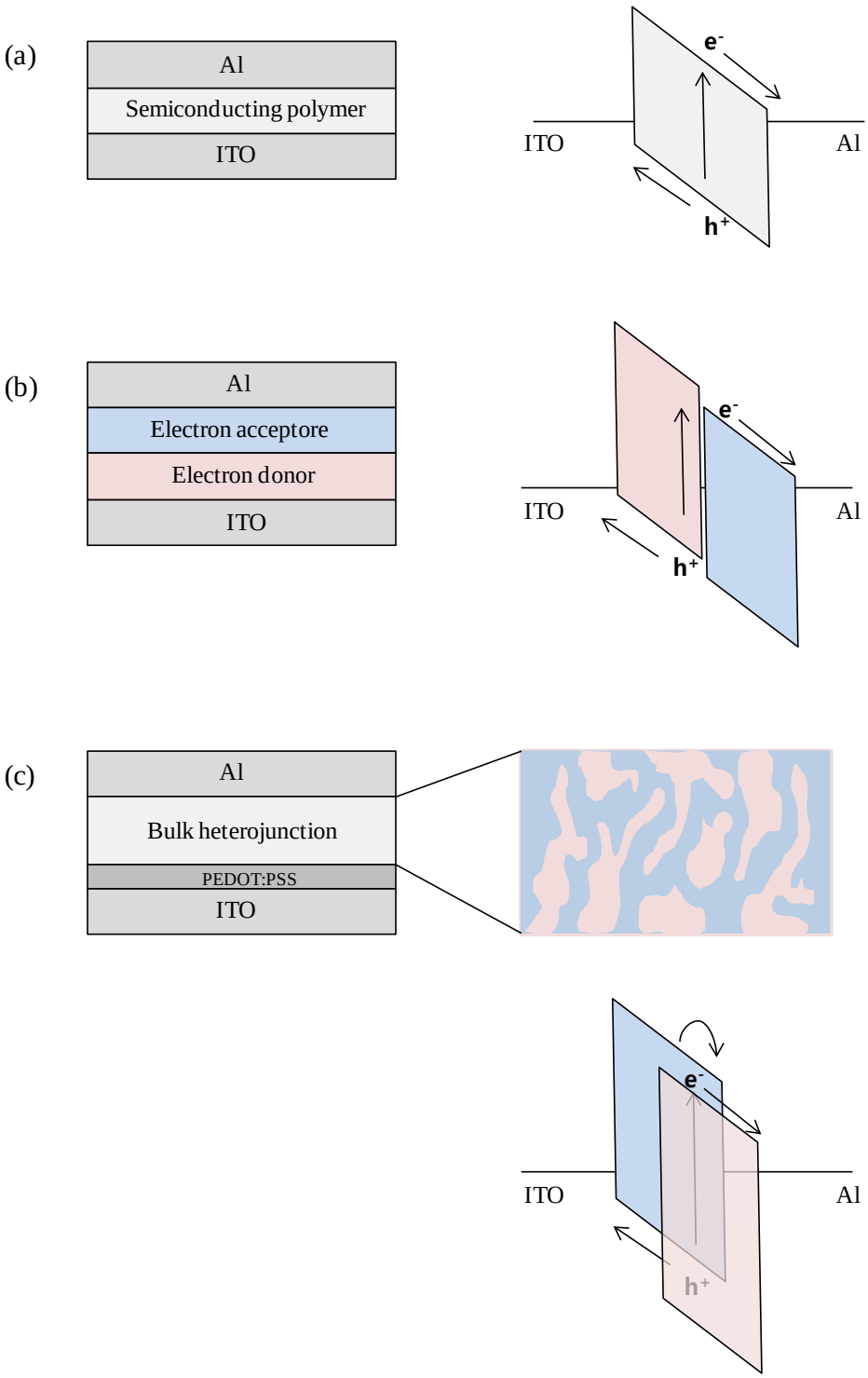

Figure 2.3. Structures and working schemes of (a) single layer, (b) bilayer, and (c) bulk heterojunction.

2.3. Donor-Acceptor Polymers for Polymer Solar Cells

The conjugated polymers have a backbone of alternating single and double carbon bonds. The conjugated polymers which are applied to polymer solar cell have special interest due to its some advantage. The conjugated polymers can apply to all polymer devices. Furthermore, it is possible to use solution process such as spin coating, doctor blade, and screen printing for thin film fabrication. Besides, solution process is an easy way to form a blend of materials.

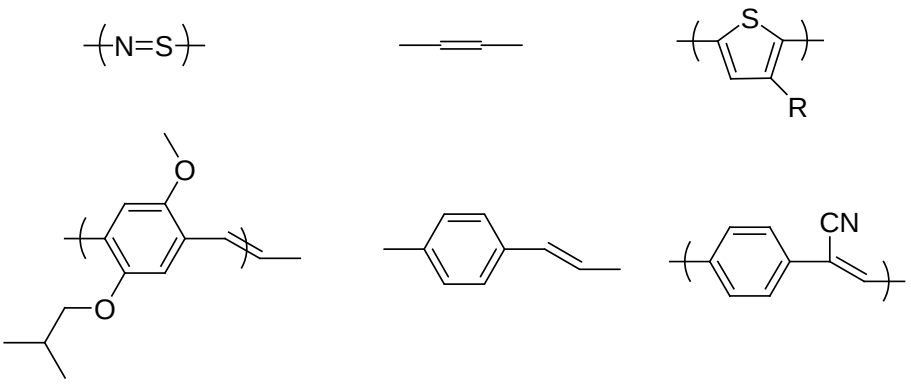

Figure 2.4. Conjugated polymers for polymer solar cells.

Generally, the optical bandgap of the conjugated polymers is around 2 eV. It is higher than the optical bandgap of silicon. Considerably higher bandgap limits light harvesting and power conversion efficiency of polymer solar cells. For example, P3HT based polymer solar cell device exhibited lower efficiency of 7.2% than that of silicon solar cell due to larger bandgap. To enhance efficiency of polymer solar cells up to 10%, it is necessary to controlling of HOMO and LUMO energy levels and the bandgap of polymers.

Figure 2.5 indicates contour plot of the bandgap and the LUMO energy level of donor polymer, and the contour lines are constant power conversion efficiency. The straight lines define the constant HOMO energy level of -0.57 and -4.8 eV. The range of LUMO energy level is -3 ~ -4 eV. The energy difference of 0.3 eV between LUMO of the donor polymer and LUMO of acceptor is enough for

charge separation [32]. Figure 2.5 implies that efficiency is more sensitive to changes of LUMO energy level than bandgap of donor polymer. To achieve 10% of energy conversion efficiency of polymer solar cells, the donor polymer should have a bandgap < 1.74 eV, and the LUMO energy level < -3.92 eV.

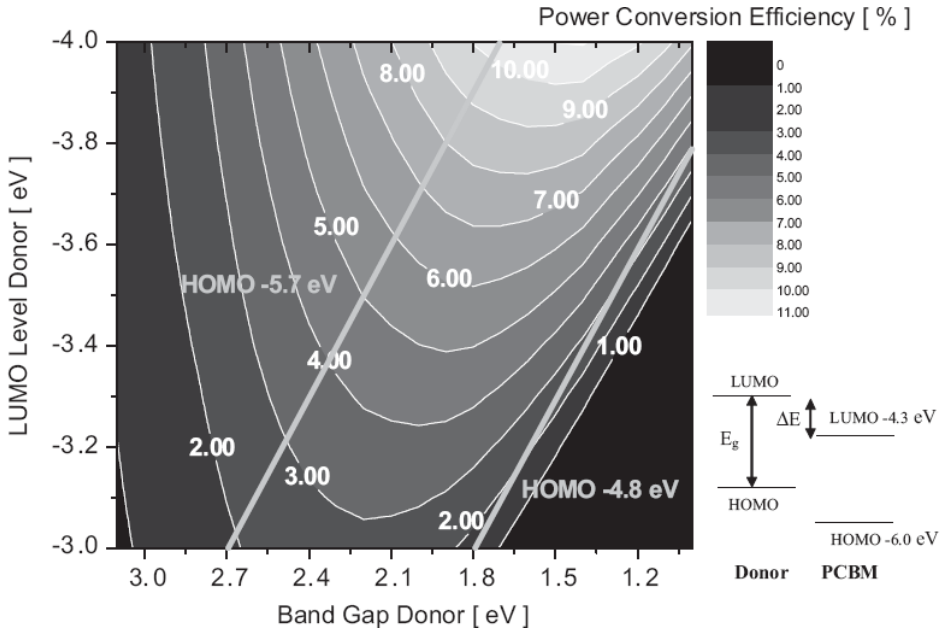

Figure 2.5. Contour plot showing the calculated energy-conversion efficiency versus the bandgap and the LUMO energy level of the donor polymer according, and a schematic energy diagram of a donor and PCBM [20].

Recent used polymers which are used as donor materials of polymer solar cells have weak donor-strong acceptor alternating architecture. The new types of conjugated polymers with donor-acceptor alternating architecture are necessary to reduce bandgap of polymer, and enhance the optical and electrochemical properties because the built-in intramolecular charge transfer facilitates control of the electronic structure [29, 33, 34]. Generally, electron rich units are used as electron donor such as fluorene, dibenzosilole, and benzodithiophene, while electron deficient units are used as electron acceptor such as benzothiadiazole, diketopyrrolopyrrole.

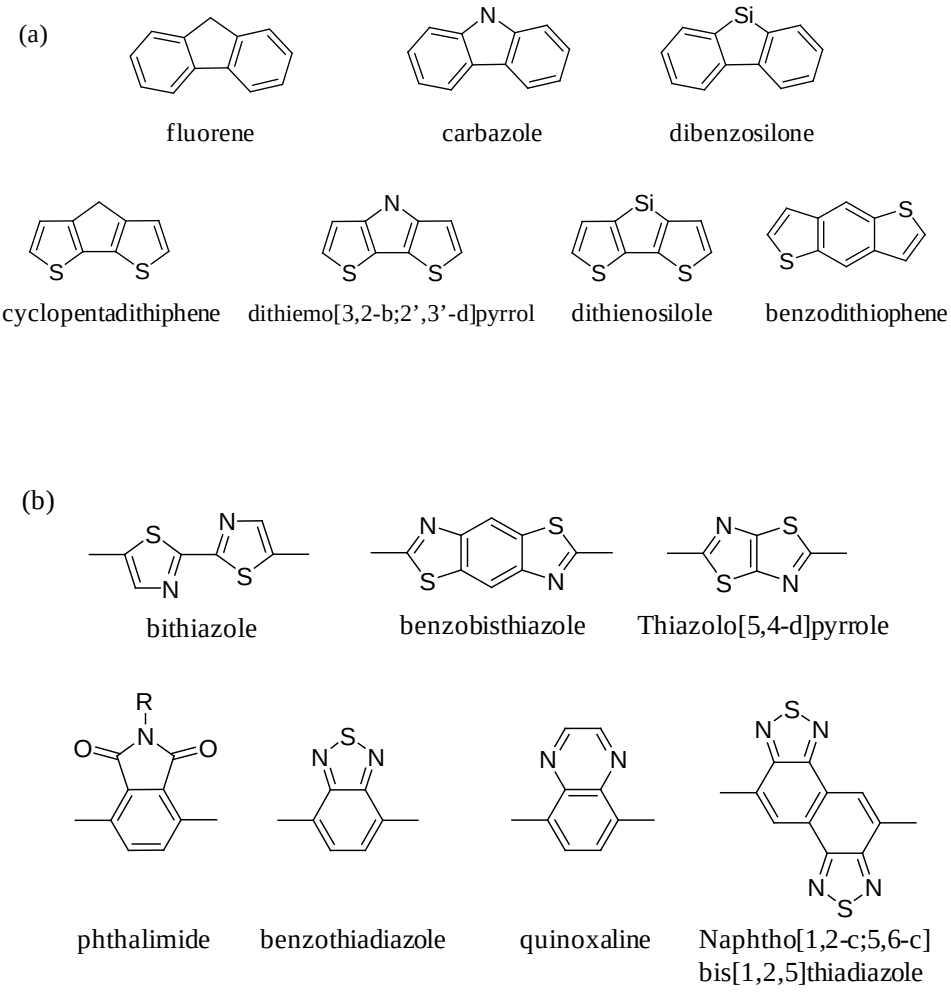

Figure 2.6. Typical donor units (a) and acceptor units (b) for donor-acceptor conjugated polymers.

The weak donor maintains a low HOMO energy level. On the other hand, the strong acceptor can reduce the gap via internal charge transfer [35].

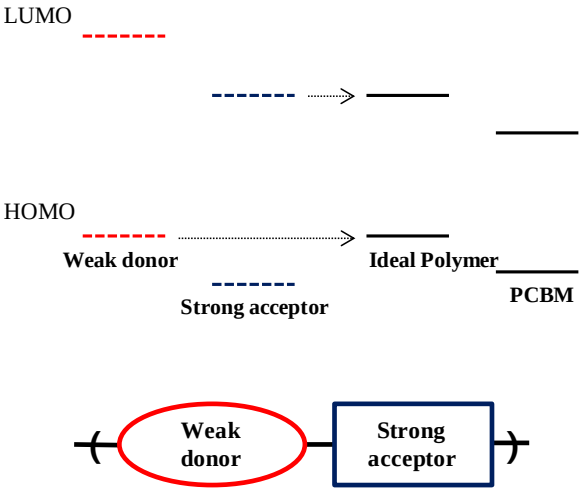

Figure 2.7. Weak donor and strong acceptor concept and energy levels.

The bandgap of conjugated polymers is ascribed to four contributions related to the conjugated polymer backbone [19].

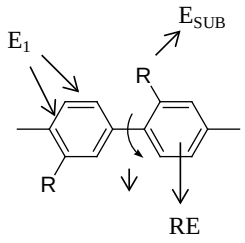

Figure 2.8. Influences of the chemical structure and conformation on the bandgap of the conjugated polymer, poly-*para*-phenylene.

(i) Bond length alternation (E_1)

Potential energy is function of bond length alternation. In the polymers with non-degenerate ground state, polymers show the difference energy which indicates an aromatic and a quinoid form. Control of the bond length can control the bandgap.

(ii) Aromaticity (RE)

Most conjugated polymers have aromatic units. Therefore, the aromaticity is one of important factor in the polymer structure. The aromaticity means the energy difference between the aromatic structure and a hypothetical reference which is consisted isolated double bonds. Aromaticity leads to a confinement of the π-electron on the ring and competes with the delocalized electrons.

(iii) Conjugation length (E_{ROT})

The longer conjugation polymer backbone shows the smaller bandgap of polymer. Torsion between adjacent aromatic rings can hinder the conjugation of polymer and lead to increase of the bandgap.

(iv) Substituent effects (E_{SUB})

Substituents give mesomeric and inductive effects. Therefore, It can change the energetic position of the HOMO or LUMO energy level. The HOMO energy level can be increased by introduction of electron-donating group to the conjugated polymer backbone. On the other hand, electron-withdrawing substituents reduce the LUMO energy of polymer.

Furthermore, intermolecular interactions can influence the bandgap in the solid state. The bandgap of conjugated polymer in the solid state is lower than that of conjugated polymer in the solution due to an increased interaction between the polymer chains. Moreover, mesoscopically ordered phases of polymer occurs in the solid state, lead to decrease of the bandgap. Bulky side chain interrupts intermolecular interaction between the polymer backbones.

2.4. Improvement of Performance of Polymer Solar Cells

2.4.1. Improvement of Light Absorption

A poor light absorption is one of the factors which limit performance of polymer solar cells. The bandgap of 1.85 eV absorbs only 46% of photon. In the case of silicon solar cells, the bandgap of 1.1 eV can absorb more than 90% of photon. The matched bandgap of polymer with the solar spectrum prevents the optical loss.

To achieve the efficiency of over 10%, the donor polymer materials should have the bandgap of below 1.7 eV. If PCBM is electron acceptor materials, LUMO energy level should be below of -3.9 eV [23]. It means that the lower bandgap polymer which alternatively uses electron donor and electron acceptor units is effective strategies to enhance absorption [36]. An attempt for synthesizing low bandgap polymer is selecting donor unit with high ionization potential and acceptor unit with high electron affinity. The commonly used donor and acceptor units are summarized in Figure 2.6.

On the other hand, the low bandgap polymers have problem. V_{oc} is determined by the difference between the LUMO energy level of the electron acceptor such as PCBM and the HOMO energy level of the electron donor as followed equation [20].

$$eV_{oc} = \left(E_{HOMO}^{donor} - E_{LUMO}^{acceptor}\right) - 0.3$$

In the low bandgap polymer, V_{oc} is lower than high bandgap polymer due to LUMO energy level of the low bandgap polymer. Therefore, reducing the LUMO energy level is suitable to maintain low bandgap and enough large V_{oc}. When deceasing bandgap, the LUMO energy and HOMO energy levels of polymer are shift from the vacuum level. Therefore, it is necessary to maintain suitable LUMO energy level for enough charge driving force for electron transfer to the electron acceptor.

2.4.2. New Device Structures

The polymer solar cells are requested a stability for commercialization. Generally, the organic materials can be easily oxidized by water or oxygen. Furthermore, acidic PEDOT:PSS is damaging to organic active layer. The low workfunction metal cathode can be easily oxidized by air. It causes short lifetime, and reduced efficiency. Therefore, an encapsulation is necessary to increase stability of polymer solar cells [37]. But the metal cathode can be oxidized even with the encapsulation. An inverted structure of polymer solar cells can overcome above limitation of stability.

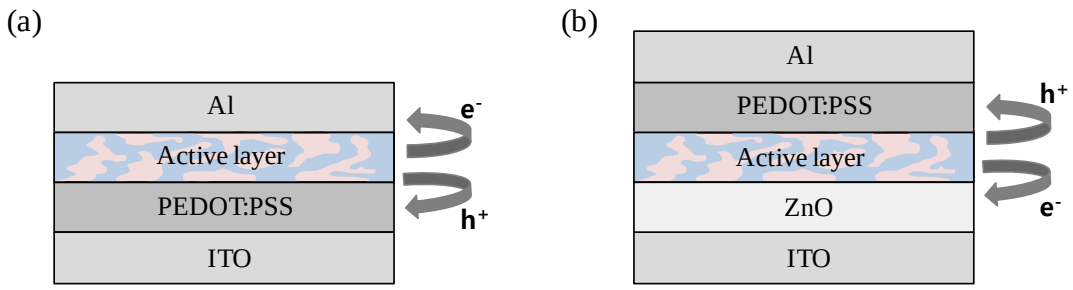

Figure 2.9. (a) Normal structure, and (b) inverted structure of polymer solar cell.

Another requested device structure is tandem structure to improve performance of polymer solar cells. The electron donor polymers have the specific bandgap and absorb limited light spectrum. The tandem structure supplements limited sunlight absorption and enhances sunlight harvesting. The stacking of double layer can absorb broad range of light spectrum because each polymer harvests different range of spectrum. Figure 2.10 shows incident photon conversion efficiency of tandem cell and structure. However, there are interfacial layer problems. The interfacial layer must collect electrons from the front cell and holes from the back cell. If there are no balance between the electrons and holes at the interfacial layer, charges accumulate and it causes reduced performance of tandem solar cells.

(a)

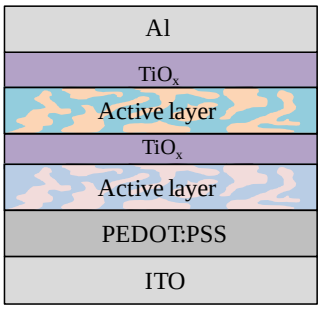

(b)

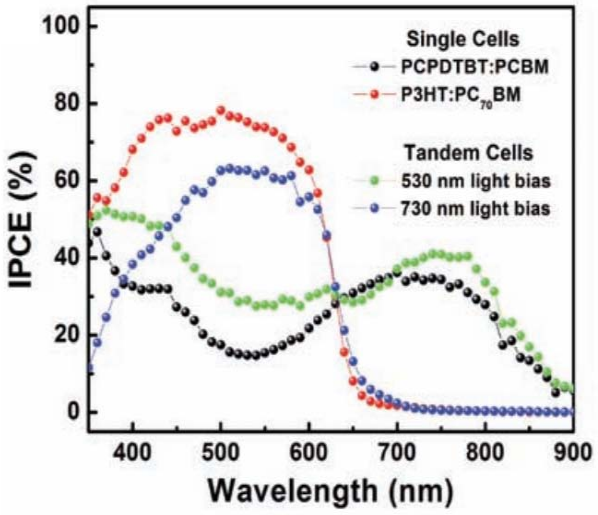

Figure 2.10. (a) Structure, and (b) incident photon conversion efficiency of tandem cell [38].

3. EXPERIMENTAL

3.1. Synthesis of Materials

3.1.1. Synthesis of Monomers

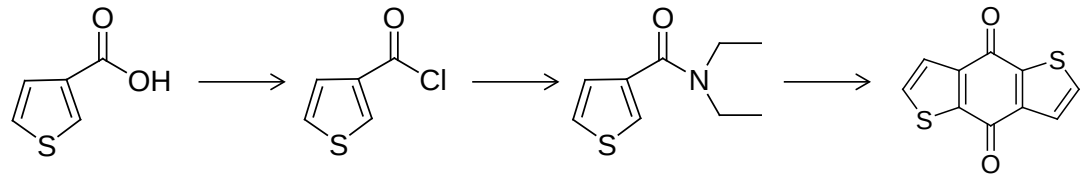

1 **2** **3**

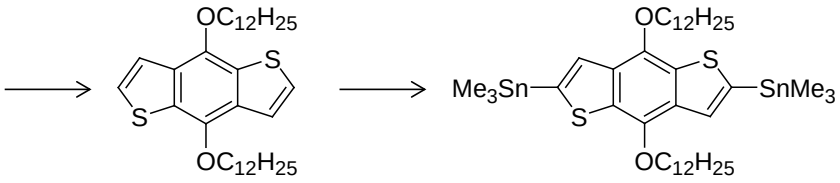

4 **5**

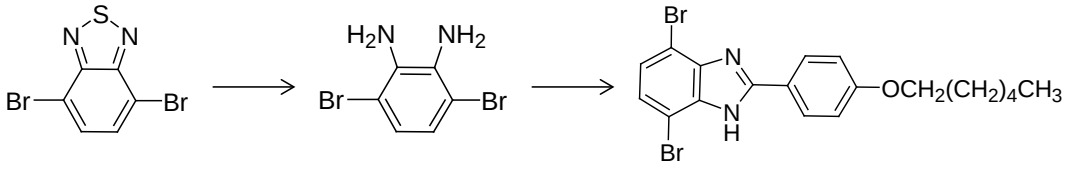

6 **7**

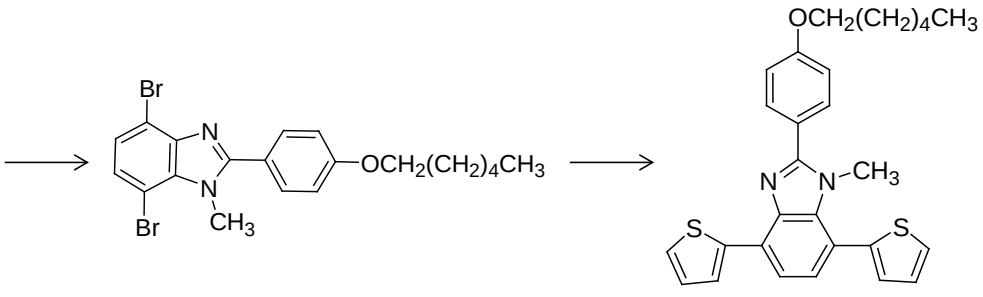

8 **9**

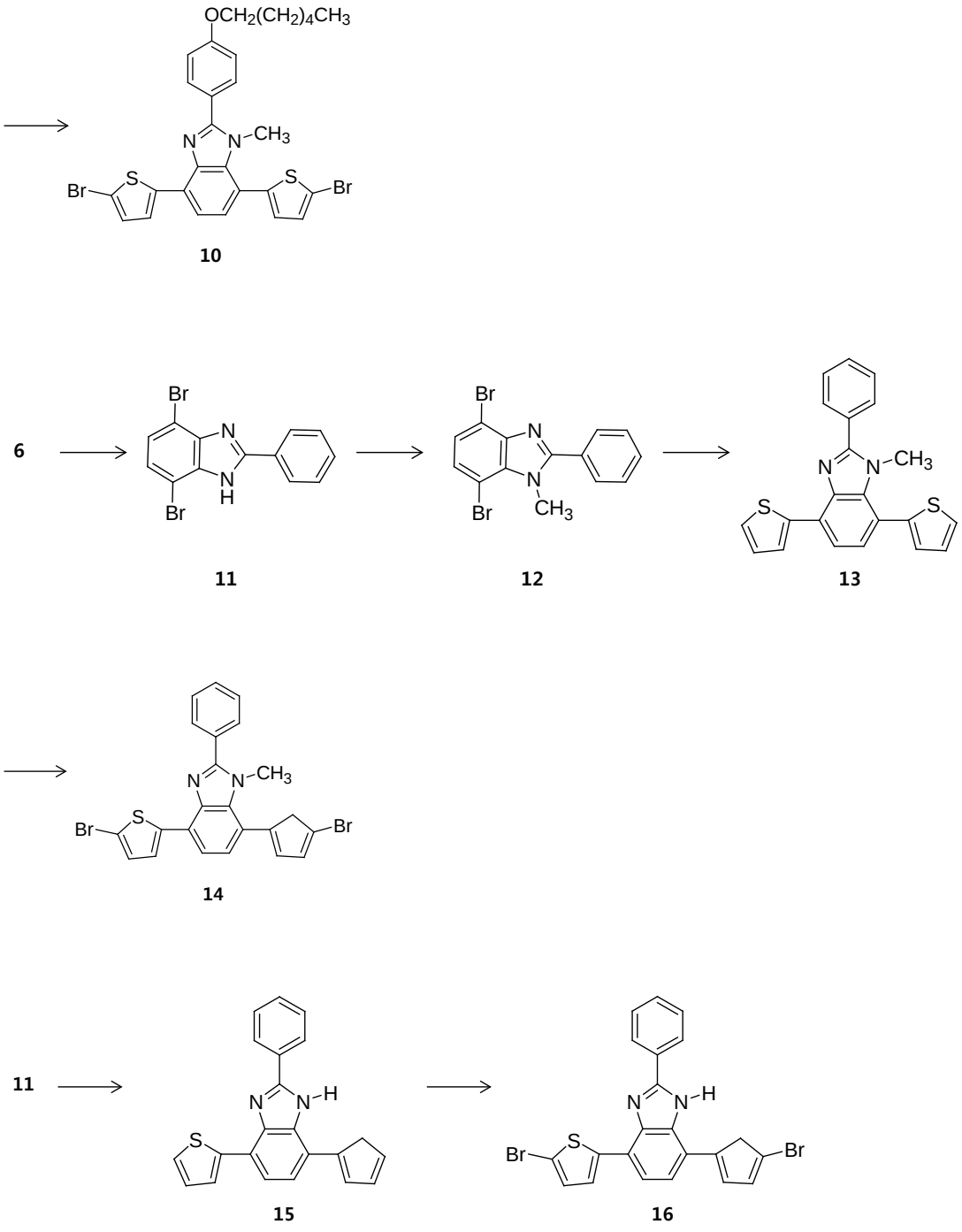

Scheme 3.1. Synthesis of benzodithiophene segment and benzimidazole segments.

3-Thiophenecarbonyl chloride (1).

3-Thiophenecarboxylic acid (5 g, 0.039 mol) was added to a round bottom flask equipped with a reflux condenser. Thionyl chloride (25 mL) was added, and the mixture was allowed to reflux for 4 hours under a blanket of nitrogen. The excess thionyl chloride was distilled, and the solution was dried on a vacuum line to yield colorless crystals.

N,N-Diethylthiophene-3-carboxamide (2).

Compound 1 was dissolved in methylene chloride (20 mL) and added dropwise at 0 ℃ to a diethylamine (8.1 mL, 0.078 mol). Solution was stirred at RT for several hours. And then, solution poured into water and extracted with methlylene chloride. The solution was dried over anhydrous sodium sulfate and evaporated to give a brown oil (6.37g, 89%). ^{1}H NMR ($CDCl_3$, 400 MHz), δ (ppm): 7.48 (s, 1H), 7.32 (d, 1H), 7.20 (d, 1H), 3.41 (m, 4H), 1.19 (t, 6H).

Benzo[1,2-b;4,5-b]dithiophene-4,8-dione (3).

Compound 2 (6.37 g, 0.035 mol) was added to a 2-neck round bottom flask that was charged with dry THF (22 mL). *n*-Butyllithium (23.9 mL, 0.038 mmol, 1.6M in hexanes) was added dropwise over 30 minutes at 0 ℃. The mixture was allowed to stirring at 0 ℃ for 30 minutes and then at RT for 2 hours. The mixture was poured over ice and allowed to sit for 4 hours. The precipitate was filtered, washed with water and methanol, and the olive green product was allowed to dry in air overnight (3.14 g, 81.5%). ^{1}H NMR ($CDCl_3$, 400 MHz), δ (ppm): 7.68 (s, 2H), 7.66 (s, 2H)

4,8-Didodecyloxybenzo[1,2-b;3,4-b']dithiophene (4).

Compound 3 (1 g, 4.54 mmol) and then pour into a 18 mL of water, and zinc powder (0.68 g, 10.45 mmol) was added. The mixture was stirred for 30 minutes, and then 2.72 g, 0.068 mol of NaOH was added to the mixture. The mixture was well stirred and heated to reflux for another 1 hour. During the reaction, the color of the mixture changed from yellow to red and then to orange. Then, 1-bromododecane (3.36 g, 13.5 mmol) and a catalytic amount of tetrabutylammonium bromide were

added into the flask. After being refluxed for 2 hours, the color of the reactant should be yellow or orange. The reactant was poured into cold water and extracted by ethyl acetate. The ethyl acetate layer was dried over anhydrous sodium sulfate. After removing solvent, the crude product was purified by column chromatography using methylene chloride/ hexane (1:5) as the eluent. 3.4 g amount of compound 4 (68%) was obtained as a straw yellow crystal. ^{1}H NMR ($CDCl_3$, 400 MHz), δ (ppm): 7.47 (d, 2H), 7.35 (d, 2H), 4.27 (t, 4H), 1.87 (m, 4H), 1.55 (m, 4H), 1.26 (m, 32H), 0.88(t, 6H)

2,6-Bis(trimethyltin)-4,8-didodecyloxybenzo-[1,2-b;3,4-b]dithiophene (5).

Compound 4 (1 g, 1.8 mmol) and 25 mL of THF were added into a flask under an inert atmosphere. The solution was cooled to -78 ℃, and n-butyllithium (3.6mL, 5.76 mmol, 1.6 M in n-hexane) was added dropwise. After being stirred at -78 ℃ for 15 minutes, the mixture was kept at RT for another 4 hours. Then, trimethyltin chloride (5.76 mL, 5.76 mmol, 1 M in THF) was added in one portion at -78 ℃and stirred at -78 ℃ for 15 minutes. The cooling bath was removed, and the reactant was stirred at RT for 4 hours. Then, it was poured into cool water and extracted by diethyl ether. The organic layer was washed by water two times and then dried by anhydrous sodium sulfate. After removing solvent under vacuum, the residue was recrystallized by ethyl alcohol. 1.33 g amount of compound 5 (83%) was obtained as a needle crystal. ^{1}H NMR ($CDCl_3$, 400 MHz), δ (ppm): 7.51 (s, 2H), 4.29 (t, 4H), 1.88 (m, 4H), 1.58 (m, 4H), 1.27 (m, 32H), 0.88 (t, 6H), 0.44 (s, 18H).

3,6-Dibromobenzene-1,2-diamine (6).

To a suspension of 4,7-dibromo-2,1,3-benzothiadiazole (2 g, 6.80 mmol) in ethanol (100 mL) was added sodium borohydride (4.75 g, 0.126 mol) at 0 ℃, and the mixture was stirred for 24 hours at RT. After evaporation of the solvent, water was added, and the mixture was extracted with ethyl acetate. The extract was washed with brine and dried over anhydrous sodium sulfate. After removing solvent, the crude product was purified by column chromatography using methylene chloride/ hexane (2:1) as the eluent. 1.49 g amount of compound 6 (82%) was obtained. ^{1}H NMR ($CDCl_3$, 400 MHz), δ (ppm): 6.85 (s, 2H), 3.90 (s, 4H).

4,7-Dibromo-2-(4-hexyloxy-phenyl)-1H-benzoimidazole (7).

Compound 6 (0.5 g, 1.88 mmol) and 4-hexyloxy benzaldehyde (0.43 g, 2.07 mmol) in 10 mL of ethanol were added into a flask, and then p-toluenesulfonic acid monohydrate (0.036 g, 1.19 mmol). The mixture was refluxed for 24 hours under a nitrogen atmosphere. The solvent was removed, and water added into the mixture. The mixture was extracted with ethyl acetate. The organic phase was dried by anhydrous sodium sulfate. After removing solvent, the crude product was purified by column chromatography using ethyl acetate/ hexane (1:5). 0.48 g amount of compound 7 (56%) was obtained. ^{1}H NMR ($CDCl_3$, 400 MHz), δ (ppm): 9.42 (s, 1H), 8.04 (d, 2H), 7.35 (d, 1H), 7.22 (d, 1H), 7.20 (d, 2H), 4.03 (t, 2H), 1.82 (m, 2H), 1.47 (m, 2H), 1.37 (m, 4H), 0.92 (m, 3H)

4,7-Dibromo-2-(4-hexyloxy-phenyl)-1-methyl-1H-benzoimidazole (8).

Compound 7 (0.5 g, 1.106 mmol) was added into 15 mL of THF, and then sodium hydride (0.040 g, 1.66 mmol) and methyl iodide (0.23 g, 1.66 mmol) were added. The mixture was stirred at 40 ℃ for 4 hours. Excess solvent was removed by distillation and the mixture was washed with water, extracted with ethyl acetate. After removing solvent, the crude product was purified by column chromatography using ethyl acetate/ hexane (1:5). 0.48 g amount of compound 8 (92%) was obtained as sticky oil. ^{1}H NMR ($CDCl_3$, 400 MHz), δ (ppm): 7.65 (d, 2H), 7.35 (d, 1H), 7.22 (d, 1H), 7.03 (d, 2H), 4.11 (s, 3H), 4.03 (t, 2H), 1.82 (m, 2H), 1.47 (m, 2H), 1.37 (m, 4H), 0.92 (m, 3H)

2-(4-Hexyloxy-phenyl)-1-methyl-4,7-di-thiophen-2-yl-1H-benzoimidazole (9).

Compound 8 (0.79 g, 1.07 mmol) and (tributylstannyl) thiophene (1.20 g, 3.22 mmol) were added into toluene (20 mL). The mixture was flushed by nitrogen for 10 minutes, then 4 mol% of $Pd(PPh_3)_4$ was added into the flask. The mixture was flushed by nitrogen for 20 minutes. The mixture was heated to 110 ℃, and the reactant was stirred for 24 hours at 110 ℃ under nitrogen atmosphere. Then, the reactant was cooled down to RT and solvent was removed. The crude product was purified by column chromatography using ethyl acetate/ hexane (1:10). 0.91 g amount of compound 9 (110%) was obtained. ^{1}H NMR ($CDCl_3$, 400 MHz), δ (ppm): 8.19 (d, 1H), 7.75 (d, 2H), 7.56 (d, 1H), 7.41 (d,

1H), 7.40 (d, 1H), 7.25 (d, 1H), 7.15 (m, 3H), 7.02 (d, 2H), 4.03 (t, 2H), 3.57 (s, 3H), 1.82 (m, 2H), 1.47 (m, 2H), 1.37 (m, 4H), 0.92 (m, 3H)

4,7-Bis-(5-bromo-thiophen-2-yl)-2-(4-hexyloxy-phenyl)-1-methyl-1H-benzoimidazole (10).

To a solution of compound 9 (0.55 g, 1.12 mol) in chloroform (50 mL) was added N-bromosuccimide (NBS) (0.43 g, 2.45 mmol) in portion. The mixture was stirred for 12 hours in the absence of light at RT. After removal of solvent, the mixture was extracted with ethyl acetate and brine. The organic layer was dried by anhydrous sodium sulfate. After removing solvent, the crude product was purified by column chromatography using ethyl acetate/ hexane (1:7). 0.54 g amount of compound 10 (76%) was obtained. ^{1}H NMR ($CDCl_3$, 400 MHz), δ (ppm): 7.73 (d, 1H), 7.71 (d, 2H), 7.47 (d, 1H), 7.26 (d, 1H), 7.09 (m, 2H), 7.02 (d, 2H), 6.91 (d, 1H) 4.03 (t, 2H), 3.57 (s, 3H), 1.82 (m, 2H), 1.47 (m, 2H), 1.37 (m, 4H), 0.92 (m, 3H)

4,7-Dibromo-2-phenyl-1H-benzoimidazole (11).

Compound 6 (0.5 g, 1.88 mmol) and 4-benzaldehyde (0.22 g, 2.07 mmol) in 10 mL of ethanol were added into a flask, and then p-toluenesulfonic acid monohydrate (0.036 g, 1.19 mmol). The mixture was refluxed for 24 hours under a nitrogen atmosphere. The solvent was removed, and water added into the mixture. The mixture was extracted with ethyl acetate. The organic phase was dried by anhydrous sodium sulfate. After removing solvent, the crude product was purified by column chromatography using ethyl acetate/ hexane (1:5). 0.24 g amount of compound 15 (36%) was obtained. ^{1}H NMR (DMSO, 400 MHz), δ (ppm): 13.30 (s, 1H), 8.33 (m, 2H), 7.57 (m, 3H), 7.38 (s, 2H)

4,7-Dibromo-1-methyl-2-phenyl-1H-benzoimidazole (12).

Compound 11 (0.5 g, 1.42 mmol) was added into 15mL of THF, and then sodium hydride (0.051 g, 2.13 mmol) and methyl iodide (0.30 g, 2.13 mmol) were added. The mixture was stirred at 40 ℃ for 4 hours. Excess solvent was removed by distillation and the mixture was washed with

water, extracted with ethyl acetate. After removing solvent, the crude product was purified by column chromatography using ethyl acetate/ hexane (1:5). 0.48 g amount of compound 16 (92%) was obtained as white solid. ^{1}H NMR ($CDCl_3$, 400 MHz), δ (ppm): 7.71 (m, 2H), 7.53 (m, 3H), 7.33 (m, 2H), 4.11 (s, 3H)

1-Methyl-2-phenyl-4,7-di-thiophen-2-yl-1H-benzoimidazole (13).

Compound 12 (0.48 g, 1.31 mmol) and (tributylstannyl) thiophene (1.47 g, 3.93 mmol) were added into toluene (20 mL). The mixture was flushed by nitrogen for 10 minutes, then 4 mol% of $Pd(PPh_3)_4$ was added into the flask. The mixture was flushed by nitrogen for 20 minutes. The mixture was heated to 110 ℃, and the reactant was stirred for 24 hours at 110 ℃ under nitrogen atmosphere. Then, the reactant was cooled down to RT and solvent was removed. The crude product was purified by column chromatography using ethyl acetate/ hexane (1:7). 0.8 g amount of compound 17 (160%) was obtained. ^{1}H NMR ($CDCl_3$, 400 MHz), δ (ppm): 8.21 (d, 1H), 7.81 (d, 2H), 7.53 (d, 1H), 7.51 (d, 3H), 7.43 (d, 1H), 7.42 (d, 1H), 7.28 (d, 1H), 7.15 (m, 3H), 3.53 (s, 3H)

4,7-Bis-(5-bromo-thiophen-2-yl)-1-methyl-2-phenyl-1H-benzoimidazole (14).

To a solution of compound 13 (0.8 g, 2.15 mmol) in chloroform (100 mL) was added N-bromosuccimide (NBS) (0.76 g, 4.69 mmol) in portion. The mixture was stirred for 12 hours in the absence of light at RT. After removal of solvent, the mixture was extracted with ethyl acetate and brine. The organic layer was dried by anhydrous sodium sulfate. After removing solvent, the crude product was purified by column chromatography using ethyl acetate/ hexane (1:7). 0.62 g amount of compound 18 (57%) was obtained. ^{1}H NMR ($CDCl_3$, 400 MHz), δ (ppm): 7.76 (d, 2H), 7.71 (d, 1H), 7.51 (m, 3H), 7.30 (d, 1H), 7.11 (d, 1H), 7.08 (s, 1H), 6.93 (d, 1H), 3.59 (s, 3H)

2-Phenyl-4,7-di-thiophen-2-yl-1H-benzoimidazole (15).

Compound 11 (0.3 g, 0.85 mmol) and (tributylstannyl) thiophene (0.95 g, 2.55 mmol) were added into toluene (20 mL). The mixture was flushed by nitrogen for 10 minutes, then 4 mol% of

$Pd(PPh_3)_4$ was added into the flask. The mixture was flushed by nitrogen for 20 minutes. The mixture was heated to 110 ℃, and the reactant was stirred for 24 hours at 110 ℃ under nitrogen atmosphere. Then, the reactant was cooled down to RT and solvent was removed. The crude product was purified by column chromatography using ethyl acetate/ hexane (1:7). 0.1 g amount of compound 15 (33%) was obtained. ^{1}H NMR ($CDCl_3$, 400 MHz), δ (ppm): 9.65 (s, 1H), 8.09 (m, 3H), 7.20 ~ 7.47 (m, 10H)

4,7-Bis-(5-bromo-thiophen-2-yl)-2-phenyl-1H-benzoimidazole (16).

To a solution of compound 15 (0.89 g, 2.48 mmol) in chloroform (100 mL) was added N-bromosuccimide (NBS) (0.96 g, 5.41 mmol) in portion. The mixture was stirred for 12 hours in the absence of light at RT. After removal of solvent, the mixture was extracted with ethyl acetate and brine. The organic layer was dried by anhydrous sodium sulfate. After removing solvent, the crude product was purified by column chromatography using ethyl acetate/ hexane (1:7). 0.35 g amount of compound 16 (27%) was obtained. ^{1}H NMR ($CDCl_3$, 400 MHz), δ (ppm): 9.45 (s, 1H), 8.12 (d, 2H), 7.89 (s, 1H), 7.52 (m, 5H), 7.48 (m, 1H), 7.14 (s, 2H)

3.1.2. Synthesis of Polymers

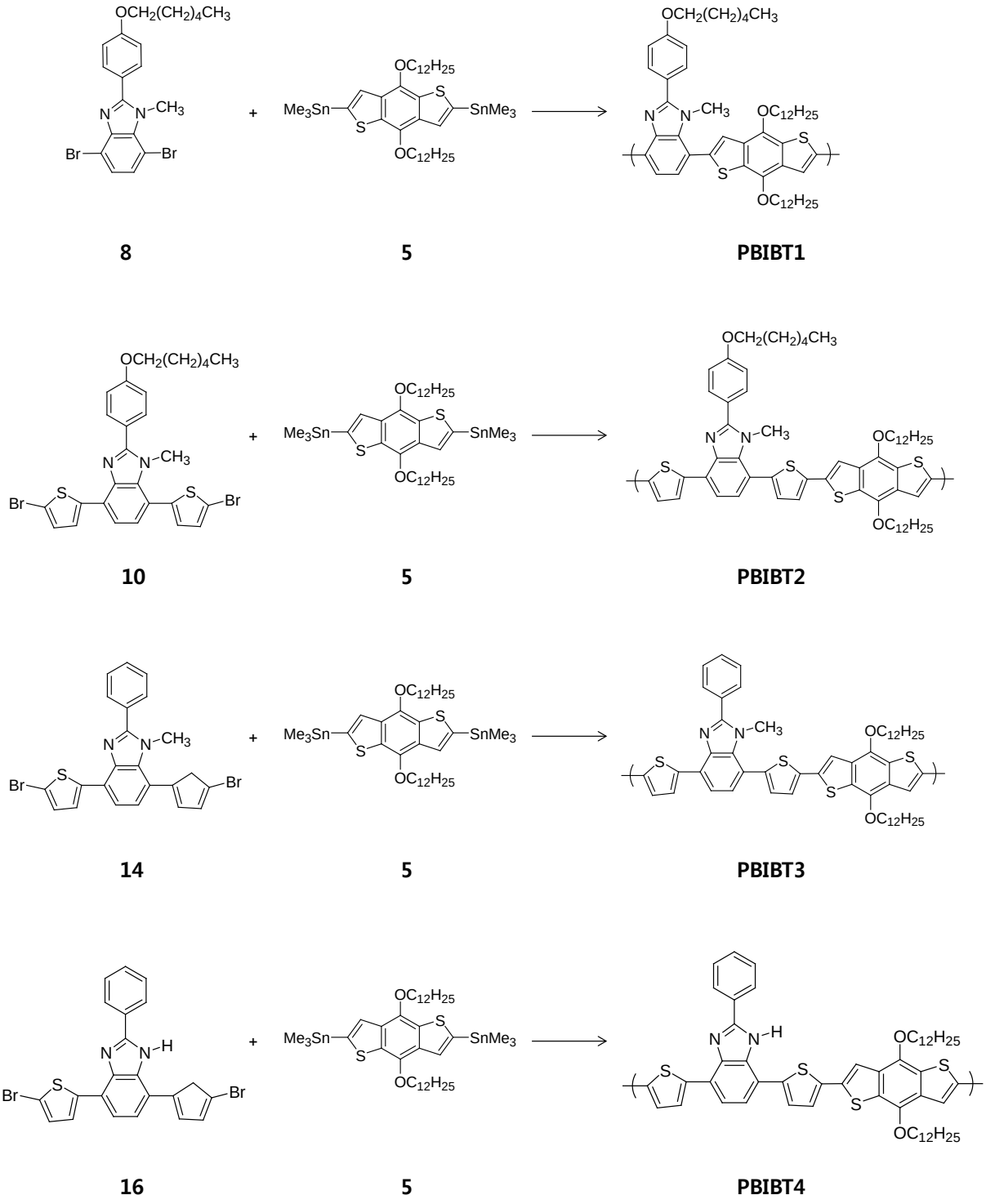

Scheme 3.2. Synthesis of polymers based on benzimidazole segments by the Stille polycondensation.

PBIBT1.

Compound 8, 4,7-Dibromo-2-(4-hexyloxy-phenyl)-1-methyl-1H-benzoimidazole (0.13 g, 0.28 mmol) and compound 5, 2,6-Bis(trimethyltin)-4,8-didodecyloxybenzo-[1,2-b;3,4-b]dithiophene (0.25 g, 0.28 mmol) were added into toluene (15 mL). The mixture was flushed by nitrogen for 10 minutes, then 4 mol% of $Pd(PPh_3)_4$ was added into the flask. The mixture was flushed by nitrogen for 20 minutes. The mixture was heated to 110 ℃, and the reactant was stirred for 24 hours at 110 ℃ under nitrogen atmosphere. Then, the mixture poured into methanol, and filtered solid. The crude product was purified by soxhlet extractor.

PBIBT2.

Compound 10, 4,7-Bis-(5-bromo-thiophen-2-yl)-2-(4-hexyloxy-phenyl)-1-methyl-1H-benzo-imidazole (0.17 g, 0.27 mmol) and compound 5, 2,6-Bis(trimethyltin)-4,8-didodecyloxybenzo-[1,2-b;3,4-b]dithiophene (0.24 g, 0.27 mmol) were added into toluene (15 mL). The mixture was flushed by nitrogen for 10 minutes, then 4 mol% of $Pd(PPh_3)_4$ was added into the flask. The mixture was flushed by nitrogen for 20 minutes. The mixture was heated to 110 ℃, and the reactant was stirred for 24 hours at 110 ℃ under nitrogen atmosphere. Then, the mixture poured into methanol, and filtered solid. The crude product was purified by soxhlet extractor.

PBIBT3.

Compound 14, 4,7-Bis-(5-bromo-thiophen-2-yl)-1-methyl-2-phenyl-1H-benzoimidazole (0.2 g, 0.38 mmol) and compound 5, 2,6-Bis(trimethyltin)-4,8-didodecyloxybenzo-[1,2-b;3,4-b]dithiophene (0.33 g, 0.38 mmol) were added into toluene (15 mL) and DMF (4 mL). The mixture was flushed by nitrogen for 10 minutes, then 4 mol% of $Pd(PPh_3)_4$ was added into the flask. The mixture was flushed by nitrogen for 20 minutes. The mixture was heated to 110 ℃, and the reactant was stirred for 24 hours at 110 ℃ under nitrogen atmosphere. Then, the mixture poured into methanol, and filtered solid. The crude product was purified by soxhlet extractor.

PBIBT4.

Compound 16, 4,7-Bis-(5-bromo-thiophen-2-yl)-2-phenyl-1H-benzoimidazole (0.2 g, 0.38 mmol) and compound 5, 2,6-Bis(trimethyltin)-4,8-didodecyloxybenzo-[1,2-b;3,4-b]dithiophene (0.34 g, 0.38 mmol) were added into toluene (15 mL) and DMF (4 mL). The mixture was flushed by nitrogen for 10 minutes, then 4 mol% of $Pd(PPh_3)_4$ was added into the flask. The mixture was flushed by nitrogen for 20 minutes. The mixture was heated to 110 ℃, and the reactant was stirred for 24 hours at 110 ℃ under nitrogen atmosphere. Then, the mixture poured into methanol, and filtered solid. The crude product was purified by soxhlet extractor.

3.2. Fabrication of Devices

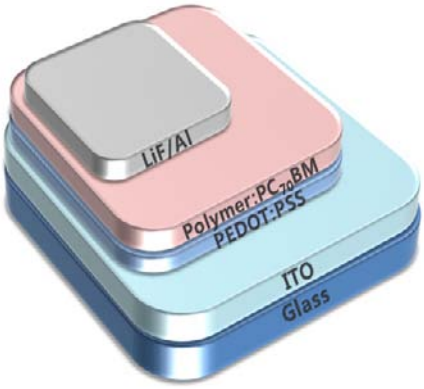

Figure 3.1. Device structure of PSCs.

Polymer solar cells were fabricated on an indium tin oxide (ITO) coated glass substrate (12 Ω/sq) with the following structure: ITO coated glass/ poly(3,4-ethylenedioxythiophene) (PEDOT:PSS)/ PBIBT:$PC_{70}BM$/ LIF/ Al. The Substrates were cleaned stepwise in acetone, di water, and isopropyl alcohol under ultrasonication for 10 minutes each. The substrates were dried in an oven. The dried substrates were treated in UV-ozone cleaner for 20min. The thin layer (30 ~50 nm) of PEDOT:PSS which was aqueous solution was spin coated onto the ITO surface. The coated substrate was baked for 20 minutes at 150 ℃. The solutions containing a mixture of PBIBT: $PC_{70}BM$ (weight ratio of 1:1, 1:2, 1:4) of 25 mg in dichlorobenzene solvent of 1mL were spin-coated on top of the PEDOT:PSS layer. The active layer film of 100 nm was dried for 1 hour at 50 ℃, then annealed for 10 min at 100 ℃. Then, LiF (1 nm) hole blocking layer and Al (100 nm) electrode were deposited by thermal evaporation in a vacuum.

3.3. Measurement and Characterization

^{1}H NMR spectra was acquired from AVANCE Ⅲ 400, Bruker, 400MHz spectrometer. $CDCl_3$ and DMSO-d_6 were used as solvents for NMR analysis. Tetramethylsilane was used as an internal reference. Molecular weights of the polymers were measured by gel permeation chromatography (GPC) method on Waters e2695 with tetrahydrofuran (THF) as an eluent. The concentration of samples was 0.5 mg/mL, which were filtered prior to the analysis. The molecular weights were calculated according to relative calibration with polystyrene as reference. UV/Vis absorption spectra were recorded on Agilent spectrometer model CARY5000. Absorption spectra measurements of the polymer solution were carried out in chloroform at 25 ℃ in quartz cuvettes. Absorption spectra measurements of the polymer films were carried out on the glass substrates with the spin-coated polymer films from the polymer solutions in dichlorobenzene. The coated substrates were annealing at 100 ℃ for 10 minutes. The electrochemical cyclic voltammetry was conducted Biologic VSP Potentiostat with a glassy carbon, Pt wire, and Ag/AgCl electrode as the working electrode, counter electrode, and reference electrode with scan rate of 100 mV/s at room temperature. Tetrabutylammonium hexafluorophosphate (Bu_4NPF_6) in acetonitrile solution 0.1 mol/L was used as electrolyte. Polymer thin films were formed by drop-casting of polymer solution in chloroform on the working electrode and dried under N_2 gas. The energy level of the Ag/AgCl reference electrode was calibrated by the Fc/Fc^+ redox system. Current-voltage characteristics were measured using Mcscience Inc. K-3300 in air without encapsulation of the cell under 1 sun (AM 1.5G) condition at 100 mW/cm^2.

4. RESULT AND DISCUSSION

4.1. Physical Properties of Polymers

Electron-deficient benzimidazole segments were synthesized by acid catalyzed cyclization reaction of 3,4-Dibromo-benzene-1,2-diamine. The benzimidazole monomers were copolymerized with trialkylstannyl substituted benzodithiophene monomers using the Stille polycondensation reaction [39, 40]. The general synthetic routes toward the polymer are outlined in Scheme 3.2. Four polymers (PBIBT1 ~ PBIBT4) with the structural variation were synthesized. A benzimidazole segment was directly coupled with benzodithiophene segment to afford PBIBT1 which has methyl substituted amine and 2-hexyloxyphenyl substituents on the benzimidazole segment. A thiophene bridge between the benzimidazole and benzodithiophene segments was introduced for PBIBT2, PBITB3, and PBIBT4. In order to adjust electronic properties of the polymers, PBIBT2, PBIBT3, and PBIBT4 were synthesized with different substituents. PBIBT3 possesses a methyl substituted amine with 2-phenyl substituent whereas PBIBT4 has an unsubstituted amine on the benzimidazole segment.

Table 1 summarizes gel permeation chromatography (GPC) results of the polymers including number-average molecular weight (M_n), weight-average molecular weight (M_w), and polydispersity index (PDI) of polymers. The polymers have M_n of 6,012 ~ 10,148, M_w of 9,313 ~ 15,865 with PDI of 1.43 ~ 1.84. PBIBT1 and PBIBT2 are readily soluble at room temperature in organic solvents such as chloroform, tetrahydrofuran, and dichlorobenzene because they possess a hexyloxy side chain on benzimidazole segment. However, PBIBT3 and PBIBT4 exhibit limited solubility in dichlorobenzene due to the lack of alkyl side chain on the benzimidazole segment. The different solubility of each polymer can affect to fabrication process of solar cell device and performance of PSCs.

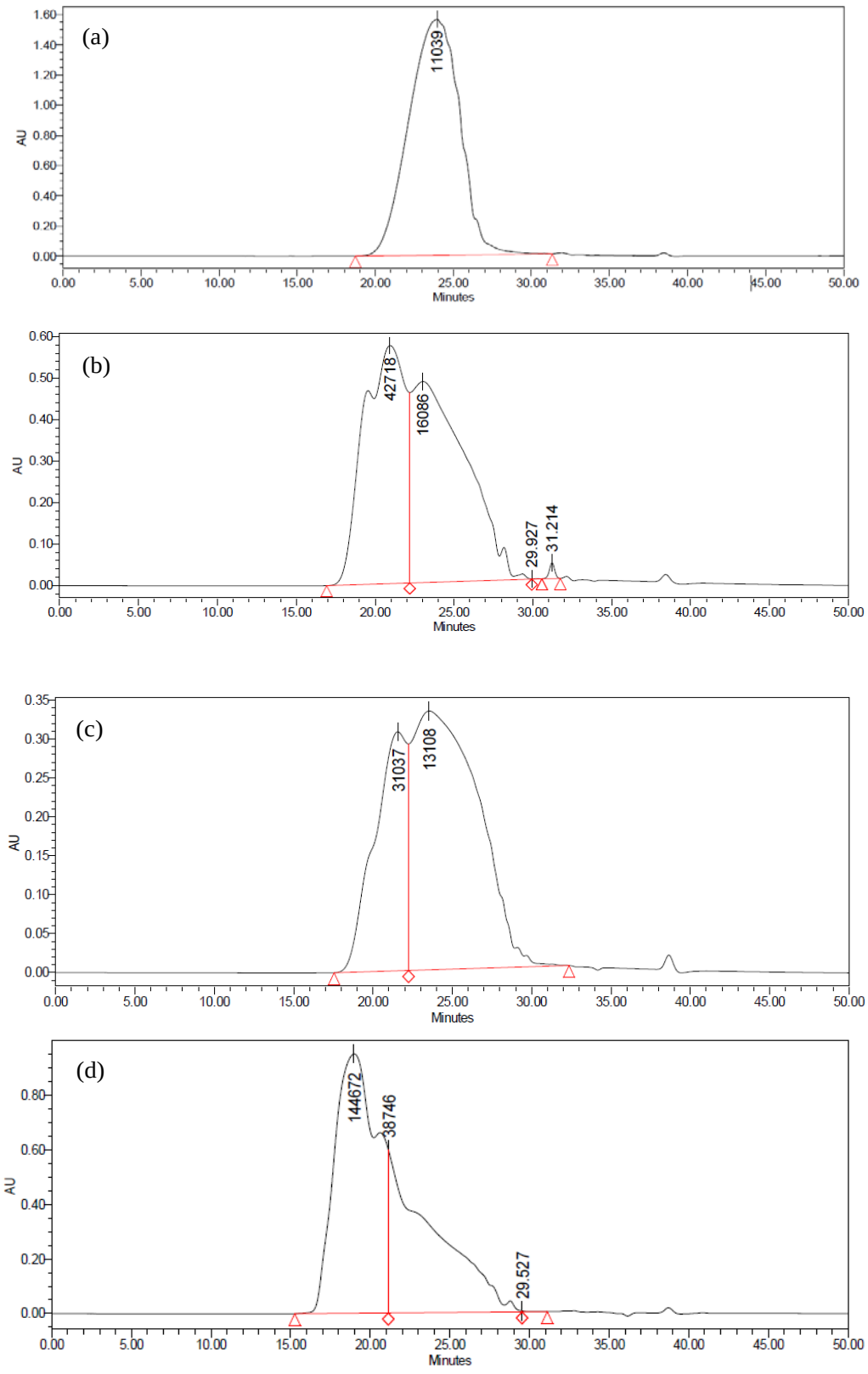

Figure 4.1. Gel permeation chromatography of polymers for molecular weights; (a) PBIBT1, (b) PBIBT2, (c) PBIBT3, (d) PBIBT4.

Table 4.1. Gel permeation chromatography (GPC) results of PBIBT polymers

Polymer	weight-average molecular weight (M_w)	number-average molecular weight (M_n)	polydispersity index (PDI)
PBIBT1	14562	10148	1.43
PBIBT2	10529	7113	1.48
PBIBT3	9313	6012	1.5
PBIBT4	15865	8599	1.84

4.2. Optical Properties of Polymers

The UV/Vis absorption spectra of PBIBT1 ~ PBIBT4 in solution and films are shown in Figure 4.2. The polymer solution was prepared in chloroform and the thin film was prepared by spin-coating dichlorobenzene solution of polymers on a glass substrate. In the absorption spectra of solution, the polymers exhibited strong absorption peak around 400 nm presumably due to a delocalized excitonic π-π^* transition in the polymer backbones [41]. The maximum absorption bands of the polymers are observed around 500 nm which is assigned to the intramolecular charge transfer (ICT) between the benzimidazole and benzodithiophene segments. PBIBT1 exhibits a maximum absorption wavelength at 429 nm and an onset absorption wavelength at 497 nm, corresponding to the optical bandgap of 2.49 eV. Compared to PBIBT1, it was found that UV/Vis absorption spectra of PBIBT2 and PBIBT3 polymers are red-shifted by 10 nm because a thiophene bridge between benzodithiophene and benzimidazole segments extends a conjugation length. In addition, PBIBT4 exhibits red-shifted maximum absorption wavelength and onset absorption wavelength by 30 nm, resulting in the optical bandgap of 2.32 eV. This result clearly indicates that the intramolecular charge transfer in PBIBT4 with a hydrogen atom on the benzimidazole segment is stronger than other polymers with a methyl substituent because the hydrogen atom on the benzimidazole segment in PBIBT4 can enhance electron-accepting property of the benzimidazole segment.

The absorption spectra in film states were similar to their corresponding absorption spectra in solution. The absorption spectra in film exhibited longer maximum absorption peak and onset wavelength. The red-shift absorption wavelength in film states was ascribed to intermolecular interaction in solid state of polymers [42].

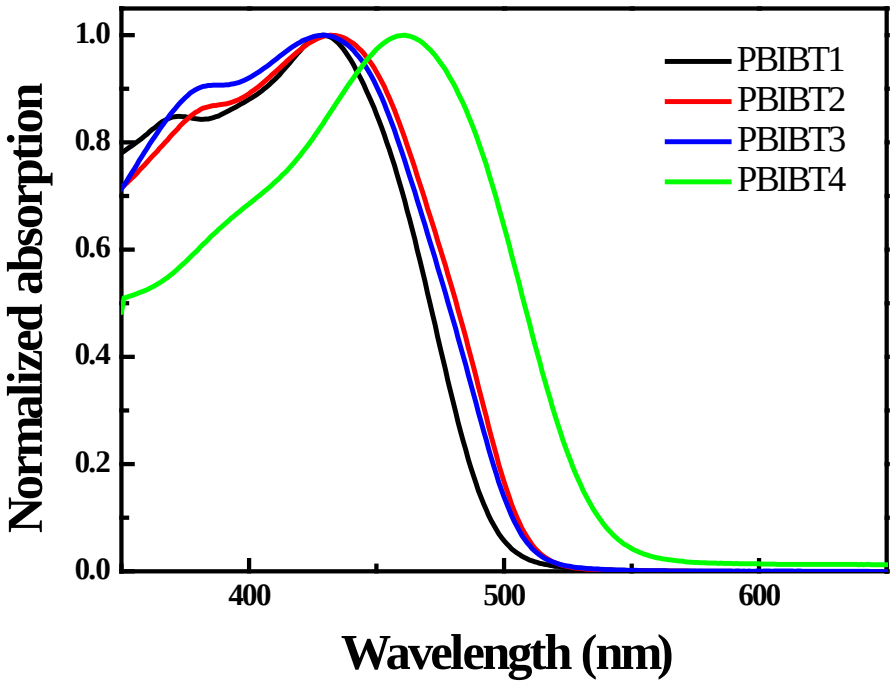

(a)

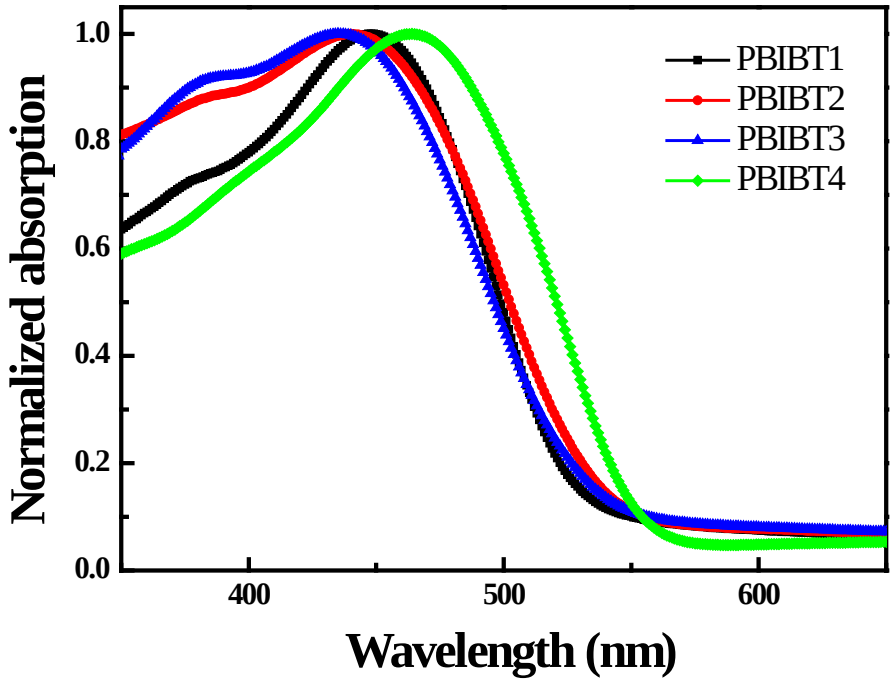

(b)

Figure 4.2 . UV/Vis absorption spectra of the polymers in solution (a) and solid films (b) on a glass.

Table 4.2. Optical properties of polymers in chloroform and films on a glass

Polymer	λ_{abs} in $CHCl_3$ (nm)	λ_{onset} in $CHCl_3$ (nm)	E_g^{opt} (eV)	λ_{abs} in films (nm)	λ_{onset} in films (nm)	E_g^{opt} (eV)
PBIBT1	429	497	2.49	447	526	2.36
PBIBT2	432	510	2.43	440	540	2.29
PBIBT3	429	508	2.44	435	533	2.32
PBIBT4	460	534	2.32	464	552	2.24

4.3. Electrochemical Properties of Polymers

Cyclic voltammetry (CV) measurement was used to investigate electrochemical properties of the polymers such as the energy levels of HOMO and LUMO as well as electrochemical bandgaps. Electrochemical properties of the polymers are summarized in Table 4.3. The HOMO and LUMO energy levels of the polymers were calculated from the onset oxidation and reduction potentials according to the following equation [43].

$$\text{HOMO (LUMO) (eV)} = -4.8 - (E_{onset} - E_{\frac{1}{2}}(\text{Ferrocene}))$$

The oxidation onsets of PBIBT1 ~ PBIBT4 are 1.72, 1.40, 1.65, and 1.60 V, corresponding to HOMO energy levels of -6.05, -5.75, -6.0, and -5.95 eV, respectively. It is well known that an open circuit voltage (V_{oc}) in a polymer solar cell is determined by the energy gap between HOMO level of electron-donor polymer and LUMO level of electron-acceptor PCBM. Therefore, it is expected that open circuit voltage (V_{oc}) values for solar cell devices based on these polymers may be enhanced due to the low-lying HOMO energy values compared to conventional P3HT polymer (-5.1 eV of HOMO energy value). The LUMO energy levels of PBIBT1 ~ PBIBT4 are estimated to be around -3.60 eV. The reduction onsets of the polymers are -0.75, -0.90, -0.73, and -0.73 V, resulting in LUMO energy levels of -3.60, -3.45, -3.62, and -3.62 eV, respectively. The electrochemical bandgap values of the polymers calculated from CV are 2.45, 2.30, 2.38, 2.33 eV, indicating that these values are in good agreement with the optical energy bandgap values. These results clearly demonstrate that the electrochemical properties of the polymers can be tuned by changing the molecular structure of the polymers. PBIBT2 exhibits slightly lower electrochemical bandgap than PBIPT4, which is caused by lower ICT effect contributed by low molecular weight of PBIBT2 than that of PBIBT4 [41]. Furthermore, the lower bandgaps of optical and electrochemical of PBIBT4 are caused by the good stacking ability of non substituted hydrogen atom with a hexyloxy long side chain.

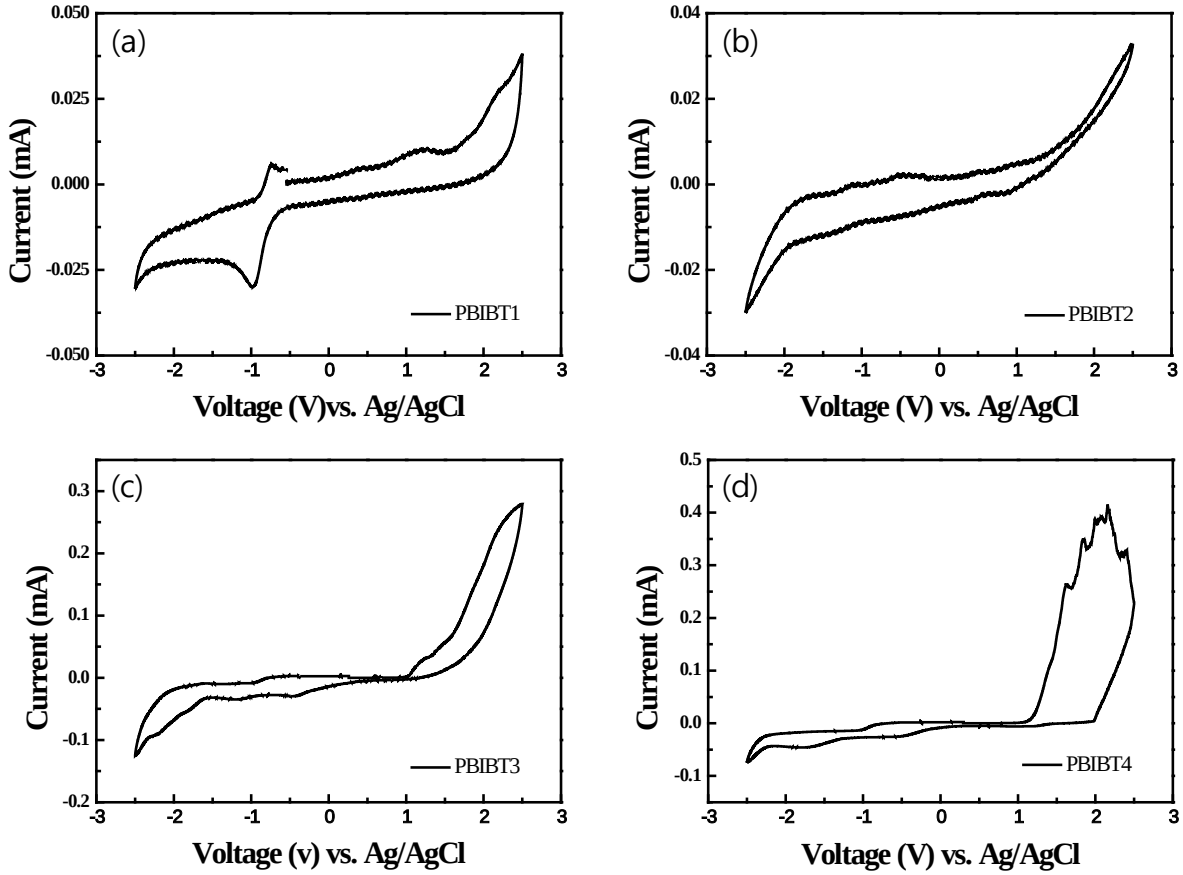

Figure 4.3. Electrochemical cyclic voltammetry curves of polymers.

Table 4.3. Electrochemical potentials and energy levels of PBIBT polymers

Polymer	E_{ox}^{onset} (V)	E_{HOMO} (eV)	E_{red}^{onset} (V)	E_{LUMO} (eV)	E_g (eV)
PBIBT1	1.72	-6.05	-0.75	-.3.60	2.45
PBIBT2	1.4	-5.75	-0.90	-3.45	2.30
PBIBT3	1.65	-6.0	-0.73	-3.62	2.38
PBIBT4	1.60	-5.95	-0.73	-3.62	2.33

4.4. Photovoltaic Properties of Polymers

In order to investigate photovoltaic performance of the polymers as electron donors, the bulk heterojunction polymer solar cell devices were fabricated with a structure of glass/ ITO/ PEDOT:PSS/ polymer:$PC_{70}BM$/ LiF:Al. Figure 4.4 shows the current density-voltage (J-V) characteristics of bulk heterojunction polymer solar cells with the polymers under AM 1.5G illumination (100 $mWcm^{-2}$). Representative characteristics of the polymer solar cells such as open circuit voltage (V_{oc}), short circuit current (J_{sc}), fill factor (FF), and power conversion efficiency (PCE) are summarized in Table 4.4. It was observed that increasing w/w ratios of $PC_{70}BM$ from 1:1 to 1:4 in the solar cell devices with all the polymers enhance the J_{sc} and FF, resulting in the improved PCE values. Using a low fullerene ratio in the blend leads to a reduction in J_{sc} due to the inefficient charge separation and transport property, resulting in relatively low PCE [44]. For instance, PCE values of solar cell devices with PBIBT3 increases from 0.05% to 0.74% when w/w ratios of $PC_{70}BM$ from 1:1 to 1:4. It was also found that PBIBT4 exhibits best solar cell with V_{oc} of 0.74 V, J_{sc} of 4.03 $mAcm^{-2}$, and FF of 30.2, resulting in PCE of 0.90%. Introduction of thiophene segments can increase PCEs of polymers because of the presence of more rigid thiophene segments in their polymer backbone with improve photocurrent. PBIBT1 and PBIBT2 exhibited PCEs of 0.21 and 0.18%, respectively, presumably due to low J_{sc} values. The lower PCE values of PBIBT1 and PBIBT2 might be caused by larger steric hindrance of long alkyl side chain of the polymers. The long hexyloxy side chain on benzimidazole segments can hinder π-π interaction between the polymer backbones, resulting in decrease of charge carrier mobility in the polymers [45]. Moreover, the long side chain of the acceptor unit can interrupt intramolecular charge transfer between the donor unit and the acceptor unit of polymer by the distortion of the conjugation of the backbone [46]. In addition, the long side chain is disadvantage in the construction of solar cells caused by reducing the strong interaction between donor and acceptor units leading to strong phase separation [47]. The solar cell devices based on PBIBT4 achieved a higher J_{sc} by 0.85 $mAcm^{-2}$ than corresponding PBIBT3 based solar cell device. Accordingly, the solar cell efficiency was improved from 0.74% of PBIBT3 to 0.9% of PBIBT4. These results clearly

indicate that the hydrogen and phenyl substituents in PBIBT4 play a key role in enhancing light harvesting property and efficient interpenetrating network for achieving high PCE values.

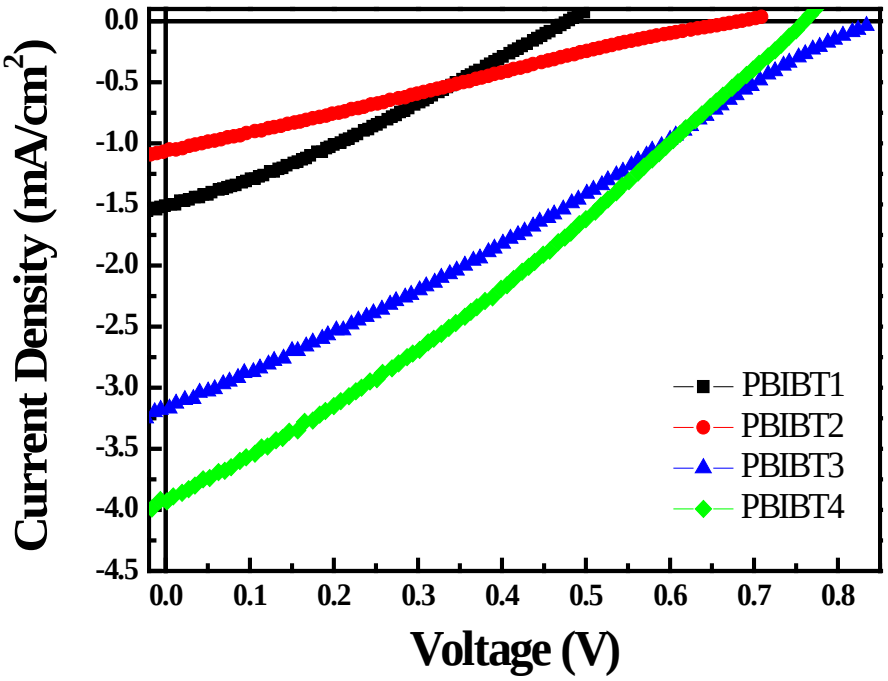

Figure 4.4. Current density-voltage (J-V) characteristics of polymer:$PC_{70}BM$ (1:4) solar cell under AM 1.5 condition.

Table 4.4. Photovoltaic properties of the PSCs with PBIBT polymers

Polymer	polymer:$PC_{70}BM$ (w:w)	V_{oc} (V)	J_{sc} (mA cm^{-2})	FF (%)	PCE (%)
PBIBT1	1:1	0.46	0.17	27.62	0.02
	1:2	0.49	1.25	24.48	0.15
	1:4	0.48	1.51	29.48	0.21
PBIBT2	1:1	0.65	0.24	22.56	0.04
	1:2	0.61	0.53	22.01	0.07
	1:4	0.68	1.06	24.68	0.18
PBIBT3	1:1	0.68	0.36	20.59	0.05
	1:2	0.82	2.02	23.8	0.4
	1:4	0.78	3.18	29.53	0.74
PBIBT4	1:1	0.79	1.91	25.32	0.38
	1:2	0.74	3.12	28.45	0.66
	1:4	0.74	4.03	30.25	0.9

5. CONCLUSION

The low bandgap of polymers is necessary to achieve high performance of polymer solar cell. To reduce bandgap of donor polymer, weak donor- strong acceptor alternating polymers are investigated. Donor-acceptor alternating polymers exhibit push-pull structure which can enhance charge carrier mobility due to the reduced interchain π-π stacking distance.

In this research, a series of copolymers with benzodithiophene segments as donor units and benzimidazole segments as acceptor units were synthesized by using the Stille polycondensation reaction. PBIBT1 and PBIBT2 have good solubility in organic solvents such as chloroform, tetrahydrofuran, and dichlorobenzene because of a hexyloxy side chain on benzimidazole segment. However, PBIBT3 and PBIBT4 exhibit limited solubility in dichlorobenzene due to the lack of alkyl side chain on the benzimidazole segment. Molecular weights of the resulting polymers were M_n of 6,012 ~ 10,148, M_w of 9,313 ~ 15,865 with PDI of 1.43 ~ 1.84 which were measured by GPC.

The optical and electrochemical properties of the resulting polymers were characterized by UV/Vis spectroscopy and cyclic voltammetry (CV). Absorption spectra of the polymer in chloroform solution exhibited two absorption bands. The absorption band at short wavelength was attributed to delocalized excitonic π-π* transition in the polymer backbones, while long wavelength was caused he intramolecular charge transfer (ICT) between the benzimidazole and benzodithiophene segments. PBIBT4 showed red-shift absorption spectrum. It caused a hydrogen atom on the benzimidazole segment which did not substitute for methyl group because the hydrogen atom in PBIBT4 can enhance electron-accepting property of the resulting polymer. Furthermore, PBIBT4 has the low optical bandgaps. The resulting polymers exhibited suitable HOMO and LUMO energy levels for photovoltaic applications. Electrochemical bandgap of PBIBT4 was lower than that of other polymers. The electrochemical bandgap values of the polymers show good matching with the optical bandgap values. These results imply that the electrochemical properties of the polymers can be tuned by changing the molecular structure of the polymers.

The efficiencies of bulk heterojunction solar cell devices increase following increasing weight

ratios of polymers and $PC_{70}BM$ from 1:1 to 1:4 due to enhanced V_{oc}, J_{sc}, FF. PBIBT1 and PBIBT2 achieved low efficiency of 0.21 and 0.18%. It might be caused by larger steric hindrance of long alkyl side chain of the polymers. PBIBT4 achieved efficiency of about 1%. Phenyl group with non long alkyl chain on benzimidazole segments of PBIBT4 affected to increase PCE. The increase efficiency indicates that the hydrogen and phenyl substituents in PBIBT4 play a key role in enhancing the optical and electrochemical properties for achieving high PCE values. This study implies that polymers containing electron-deficient benzimidazole segments can achieve high PCE through structural modification of the polymers.

REFERENCES

[1] Chen, H., Hou, J., Zhang, S., Liang, Y., Yang, G., Yang, Y., Yu, L., Wu, Y., Li, G. (2009). “Polymer solar cells with enhanced open-circuit voltage and efficiency.” *Nature Photon.*, 3, pp. 649-653.

[2] Chen, M.-H., Hou, J., Hong, Z., Yang, G., Sista, S., Chen, L., Yang, Y. (2009). “Efficient Polymer Solar Cells with Thin Active Layers Based on Alternating Polyfluorene Copolymer/Fullerene Bulk Heterojunctions.” *Adv. Mater*., 21, pp. 4238-4242.

[3] Dennler, G., Scharber, M. C., Brabec, C. J. (2009). “Polymer-fullerene bulk-heterojunction solar cells.” *Adv. Mater.*, 21, pp. 1-16.

[4] Zhou, H., Yang, L., Stoneking, S., You, W. (2010). “A Weak Donor−Strong Acceptor Strategy to Design Ideal Polymers for Organic Solar Cells.” *ACS Appl. Mater. Interfaces*, 2, pp. 1377-1383.

[5] Melzer, C., Koop, E. J., Mihailetchi, V. D., Blom, P. W. M. (2004). “Hole Transport in Poly(phenylene vinylene)/Methanofullerene Bulk-Heterojunction Solar Cells.” *Adv. Funct. Mater.,* 14, pp. 865-870.

[6] Thompson, B. C., Kim, Y., McCarley, T. D., Reynolds J. R. (2006). “Soluble Narrow Bandgap and Blue Propylenedioxythiophene-Cyanovinylene Polymers as Multifunctional Materials for Photovoltaic and Electrochromic Applications.” *J. Am. Chem. Soc.*, 128, pp. 12714-12725.

[7] Osaka, I., Shimawaki, M., Mori, H., Doi, I., Miyazaki, E., Koganezawa, T., Takimiya, K. (2012). “Synthesis, Characterization, and Transistor and Solar Cell Applications of a Naphthobisthiadiazole-Based Semiconducting Polymer.” *J. Am. Chem. Soc.*, 134, pp. 3498-3507.

[8] Lai, M.-Y., Chen, C.-H., Huang, W.-S., Lin, J. T., Ke, T.-H., Chen, L.-Y., Tsai, M.-H., Wu, C.-C. (2008). “Benzimidazole/Amine-Based Compounds Capable of Ambipolar Transport for Application in Single-Layer Blue-Emitting OLEDs and as Hosts for Phosphorescent Emitters.” *Angew. Chem. Int. Ed.*, 47, pp. 581-585.

[9] Hung, W.-Y., Chi, L.-C., Chen, W.-J., Chen, Y.-M., Chou, S.-H., Wong, K.-T. (2010). “A new benzimidazole/carbazole hybrid bipolar material for highly efficient deep-blue electrofluorescence,

yellow–green electrophosphorescence, and two-color-based white OLEDs." *J. Mater. Chem.*, 20, pp. 10113-10119.

[10] Hoppe, H., Sariciftci, N. S. (2004). "Organic solar cells: An overview." *J. Mater. Res.*, 19, pp. 1924-1945.

[11] Kim, M. (2009). "Understanding Organic Photovoltaic Cells: Electrode, Nanostructure, Reliability, and Performance." *Ph.D Thesis*, The University of Michigan, Ann Arbor, United States, 14 pages.

[12] Heremans, P., Arkhipov, V. I., Bassler, H. (2003). "Why is exciton dissociation so efficient at the interface between a conjugated polymer and an electron acceptor?" *Appl. Phys. Lett.*, 82, pp. 4605-4607.

[13] Hoppe, H., Sariciftci, N. S. (2008). "Polymer solar cells." *Adv. Polym. Sci.*, 214, pp. 1-86.

[14] Lee, S.-H. (2006). "Silicon solar cell." *Poly. Sci. Technol.*, 17, pp. 400-406.

[15] Gregg, B. A., Hanna, M. C. (2003). "Comparing organic to inorganic photovoltaic cells: Theory, experiment, and simulation." *J. Appl. Phys.*, 93, pp. 3605-3614.

[16] Spanggaard, H., Krebs, F. C. (2004). "A brief history of the development of organic and polymeric photovoltaics." *Sol. Energy Mater. Sol. Cells*, 83, pp. 125-146.

[17] Heeger, A. J. (2001). "Nobel lecture: semiconducting and metallic polymers: the fourth generation of polymeric materials." *Rev. Mod. Phys.*, 73, pp. 681-700.

[18] Barth, S., Bassler, H. (1997). "Intrinsic photoconduction in PPV-type conjugated polymers." *Phys. Rev. Lett.*, 79, pp. 4445-4448.

[19] Winder, C., Sariciftci, N. S. (2004). "Low bandgap polymers for photon harvesting in bulk heterojunction solar cells." *J. Mater. Chem.*, 14, pp. 1077-1086.

[20] Scharber, M. C., Mühlbacher, D., Koppe, M., Denk, P., Waldauf, C., Heeger, A. J., Brabec, C. J. (2006). "Design Rules for Donors in Bulk-Heterojunction Solar Cells—Towards 10 % Energy-Conversion Efficiency." *Adv. Mater.*, 18, pp. 789-794.

[21] Glenis, S., Tourillon, G., Garnier, F. (1986). "Influence of the doping on the photovoltaic properties of thin films of poly-3-methylthiophene." *Thin Solid Films*, 139, pp. 221-231.

[22] Brabec, C. J., Cravino, A., Meissner, D., Sariciftci, N. S., Rispens, M. T., Sanchez, L., Hummelen, J. C., Fromherz, T. (2002). “The influence of materials work function on the open circuit voltage of plastic solar cells.” *Thin Solid Films*, 403, pp. 368-372.

[23] Chi, W., Gong, X., Cao, Y. (2010). “Polymer solar cells: Recent development and possible routes for improvement in the performance.” *Sol. Energy Mater. Sol. Cells*, 94, pp. 114-127.

[24] Wöhrle, D., Meissner, D. (1991). “Organic solar cells.” *Adv. Mater.*, 3, pp. 129-138.

[25] Tang, C. W. (1986). “Two-layer organic photovoltaic cell.” *Appl. Phys. Lett.*, 48, pp. 183-185.

[26] Schilinsky, P., Waldauf, C., Brabec C. J. (2002). “Recombination and loss analysis in polythiophene based bulk heterojunction photodetectors.” *Appl. Phys. Lett.*, 81, pp. 3885-3887.

[27] Gebeyehu, D., Pfeiffer, M., Maennig, B., Drechsel, J., Werner, A., Leo, K. (2004). “Highly efficient p-i-n type organic photovoltaic devices.” *Thin Solid Films*, 451, pp. 29-31.

[28] Günes, S., Neugebauer, H., Sariciftcichemical, N. S. (2007). “Conjugated Polymer-Based Organic Solar Cells.” *Chem. Rev.*, 170, pp. 1324-1338.

[29] Yu, G., Gao, J., Hummelen, J. C., Wudl, F., Heeger, A. J, (1995). “Polymer Photovoltaic Cells: Enhanced Efficiencies via a Network of Internal Donor-Acceptor Heterojunctions.” *Science*, 270, pp. 1789-1791.

[30] Brabec, C. J, Sariciftci, N. S., Hummelen, J. C. (2001). “Plastic Solar Cells.” *Adv. Funct. Mater.*, 11, pp.15-26.

[31] Shaheen, S. E., Brabec, C. J., Sariciftci, N. S. (2001). “2.5% efficient organic plastic solar cells.” *Appl. Phys. Lett.*, 78, pp. 841-843.

[32] Brédas, J.-L., Beljonne, D., Coropceanu, V., Cornil, J. (2004). “Charge-Transfer and Energy-Transfer Processes in π-Conjugated Oligomers and Polymers: A Molecular Picture.” *Chem. Rev.*, 104, pp. 4971-5003.

[33] Antoniadis, H., Hsieh, B. R., Abkowitz, M. A., Jenekhe S. A., Stolka, M. (1994). “Photovoltaic and photoconductive properties of aluminum/poly(*p*-phenylene vinylene) interfaces.” *Synth. Met.*, 62, pp. 265-271.

[34] Granström, M., Petritsch, Arias, A. C., Lux, A., Andersson M. R., Friend, R. H. (1998).

"Laminated fabrication of polymeric photovoltaic diodes." *Nature*, 395, pp. 257-260.

[35] Roncali, J. (1997). "Synthetic Principles for Bandgap Control in Linear π-Conjugated System." *Chem. Rev.*, 97, pp. 173-205.

[36] Zhang, F., Mammo, W., Andersson, L. M., Admassie, S., Andersson, M. R., Inganäs, O. (2006). "Low-Bandgap Alternating Fluorene Copolymer/Methanofullerene Heterojunctions in Efficient Near-Infrared Polymer Solar Cell." *Adv. Mater.*, 18, pp. 2169-2173.

[37] Jørgensen, M., Norrman, K., Krebs, F. C. (2008). "Stability/degradation of polymer solar cells." *Sol. Energy Mater. Sol. Cells*, 92, pp. 686-714.

[38] Kim, J. Y., Lee, K., Coates, N. E., Moses, D., Nguyen, T., Dante, M., Heeger, A. J. (2007). "Efficient Tandem Polymer Solar Cells Fabricated by All-Solution Processing." *Science*, 317, pp. 222-225.

[39] Li, W., Xu, B., Li, H., Cheng, W., Xue, W. L., Chen, F., Lu, H., Tian, W. (C2011). "Molecular Engineering of Copolymers with Donor-Acceptor Structure for Bulk Heterojunction Photovoltaic Cells Toward High Photovoltaic Performance." *J. Phys. Chem.*, 115, pp. 2386-2397.

[40] Chang, C., Cheng, Y., Hung, S., Wu, J., Kao, W., Lee, C., Hsu, C. (2012). "Combination of Molecular, Morphological, and Interfacial Engineering to Achieve Highly Efficient and Stable Plastic Solar Cells." *Adv. Mater.*, 24, pp. 549-553.

[41] Song, S., Kang, I., Kin, G., Jin, Y., Kim, I., Kim, J. Y., Suh, H. (2012). "Synthesis and photovoltaic properties of copolymers based on 2,2-(1,5-pentamethylene)-2H-benzimidazole." *Synth. Met.*, 162, pp. 225-230.

[42] Wang, X., Sun, W., Chen, S., Guo, X., Zhang, M., Li, X., Li, Y., Wang, H. (2012). "Effects of π-Conjugated Bridges on Photovoltaic Properties of Donor-π-Acceptor Conjugated Copolymers." *Macromolecules*, 45, pp. 1208-1216.

[43] Horowitz, G. (1998). "Organic Field-Effect Transistors." *Adv. Mater.*, 10, pp. 365-377.

[44] Baek, N. S., Hau, S. K., Yip, H. Acton, O., Chen, K., Jen. A. K. Y. (2008). "High Performance Amophous Metallated π-Conjugated Polymers for Field-Effect Transistors and Polymer Solar Cells." *Chem. Mater.*, 20, pp. 5734-5736.

[45] Dou, L., Gao, J., Richard, E., You, J., Chen, C.-C., Cha, K. C., He, Y., Li, G., Yang, Y. (2012). “Systematic Investigation of Benzodithiophene- and Diketopyrrolopyrrole-Based Low-Bandgap Polymers Designed for Single Junction and Tandem Polymer Solar Cells.” *J. Am. Chem. Soc.*, 134, pp. 10071-10079.

[46] Song, S., Park, S. H., Jin, Y., Kim, J., Shim, J. Y., Goo, Y., Jung, O.-S., Kim, I., Lee, H., Jeong, E. D., Jin, J. S., Lee, K., Suh, H. (2011). “Synthesis and characterization of 2H-benzimidazole- and terthiophene-based polymer for organic photovoltaics.” *Synth. Met.*, 161, pp. 307-312.

[47] Song, S., Park, S., Kwon, S., Shim, J. Y., Jin, Y., Park, S. H., Kim, I., Lee, K., Suh, H. (2012). “Synthesis and Photovoltaic Properties of Polymers Based on Cyclopentadithiophene and Benzimidazole Units.” *Bull, Korean Chem. Soc.*, 33, pp. 1861-1866.

요 약 문

벤즈이미다졸을 포함하는 고분자 태양전지용 고분자의 합성 및 특성 분석

본 논문은 고분자 태양전지의 성능 향상을 위하여, 전자 부족한 특성의 벤즈이미다졸과 전자 풍부한 특성을 나타내는 벤조디싸이오펜 단위를 이용하여 고분자 태양전지에 적용가능 한 새로운 고분자의 설계 및 합성을 진행하였다. 각각의 고분자는 Stille polycondensation을 통해 합성 하였고, 합성 된 고분자의 광학적, 전기 화학적 특성은 고분자에 각각 다른 치환기를 도입해 주어 조절하였다. 알킬 사슬이 치환된 고분자는 유기 용매에 높은 용해도를 나타내었지만, 알킬 사슬이 도입되지 않은 고분자는 유기 용매에 제한된 용해도를 나타내었다. 겔 투과 크로마토그래피 (GPC)를 통한 분자량 분석에서 합성된 고분자들은 10148 ~ 6012 의 수 평균 분자량 (M_n)을 나타내었다. 합성 된 고분자의 광학적, 전기 화학적 특성을 UV/Vis 분광기 및 순화 전압 전류 곡선 (CV)을 통해서 분석하였다. 합성 된 각각의 고분자는 낮은 광학적 밴드갭과 전기 화학적 밴드갭을 나타내었다. 또한 CV 분석을 통해, 합성 된 고분자가 태양전지에 적용 적합한 HOMO 에너지와 LUMO 에너지인 -3.4 ~ 6.0 eV 범위의 에너지를 가지고 있음을 확인하였다. 이 결과, HOMO와 LUMO 에너지는 전자를 전극으로 이동하기 위해 적합한 에너지 차이를 주어, 합성 된 고분자가 높은 성능의 고분자 태양 전지에 적합 하다는 것을 예측할 수 있었다. 고분자의 광전지 특성을 분석하기 위해서, 합성 된 고분자를 적용하여 태양전지 디바이스를 제작하였다. 광전지 특성분석을 통해 벤즈이미다졸을 포함하는 고분자가 약 1%의 효율을 나타내는 것을 확인하였다. 이는 고분자 사슬에 도입된 치환기과 알킬 사슬의 변화로 인해 향상 된 빛의 흡수와 효과적인 interpenetrating network 구조로 인한 것으로 설명할 수 있다. 본 논문의 결과는 전자 부족한 벤즈이미다졸을 포함하는 고분자는 치환기의 도입을 통한 구조적인 변화로 인해 높은 효율을 얻을 수 있다는 것을 나타내고 있다.

핵심어: 고분자 태양전지, 공액 고분자, 벤즈이미다졸, 벤조다싸이오펜, 전자 주개-받게 구조

ACKNOWLEDGEMENT

대구경북과학기술원에서 대학원 학업을 시작한지 벌써 2년의 시간이 흘러 석사 과정의 마침표를 찍게 되었습니다. 부족하기만 했던 제가 이렇게 무사히 연구를 마칠 수 있었던 것은 제 주변의 많은 분들의 도움과 배려가 있었기에 가능했습니다. 이 기회를 통해 많은 분들께 감사의 말씀을 전하고자 합니다.

먼저 아무것도 모르는 부족하기만 한 제가 성장 할 수 있도록 이끌어주시고, 가르침을 아끼지 않으셨던 저의 지도교수님 이윤구 교수님께 감사의 말씀을 드리고 싶습니다. 교수님의 가르침을 통해 많은 것을 배울 수 있었습니다. 그리고 제가 학위 논문을 무사히 마칠 수 있도록 도움을 주신 에너지 연구부의 김대환 박사님, 그리고 홍승태 교수님께도 감사의 말씀을 드립니다.

또한 연구실 생활을 하면서 힘든 일이나 곤란한 일이 있을 때 거리낌없이 도움을 주고 걱정을 해준 연구실의 -영준, 일연, 동환, 홍기, 형진, 동화- 오빠들과 항상 저의 이야기를 들어주며 힘을 준 친구 유미에게도 고마움을 전하고 싶습니다. 그리고 동기생으로 입학하여 학교생활을 같이 하였던 동기 - 순욱, 원교, 승효, 준교, 동휘- 오빠들 그리고 학과 동기이자 룸메이트였던 인혜 언니에게도 역시 많은 도움을 받았고 덕분에 좋은 대학원 생활을 할 수 있었습니다. 그리고 항상 밝은 모습으로 웃음을 지을 수 있게 해준 가영이와 은영이 에게도 고마움을 전하고 싶습니다. 이 외에도 저에게 배려와 조언을 아끼지 않았던 학교, 학과의 많은 분들께 감사를 전합니다. 2년 이라는 시간 동안 많은 좋은 사람들을 만날 수 있었던 것 같아, 이 시간이 저에게 큰 의미가 될 것 같습니다.

마지막으로 어떤 모습의 저라도 항상 믿어주시고 자랑스러워 해주셨던 부모님께 감사드리며 사랑한다는 말씀을 드리고 싶습니다. 앞으로 졸업을 하고 어떤 모습으로 어떤 자리에 있든지 아버지와 어머니께서 자랑스러워 할 수 있는 딸이 되겠습니다. 그리고 저를 걱정하며 듬직한 모습으로 위안이 되어 주던 멋진 가민 언니, 지금 의경으로 군복무 중인 동생 지섭이가 있어 많은 위로를 받을 수 있었습니다. 언제나 저에게 위로가 되어 주고 힘이 되어준 가족이 있어 힘을 낼 수 있었습니다.

다시 한번 제가 2년 동안 학교 생활과 더불어 연구와 논문을 무사히 마칠 수 있게 도와주신 모든 분들께 감사의 말씀을 드립니다.